Article:
Xie, A., Georgiou, P.G., Pedersen, J.S. et al. (2026) Can a modified Kratky–Porod worm-like chain model describe weak polyelectrolyte random copolymers in dilute aqueous solution? Macromolecules. ISSN: 0024-9297

https://doi.org/10.1021/acs.macromol.6c00697

Macromolecules

pubs.acs.org/Macromolecules
Article

Can a Modified Kratky–Porod Worm-Like Chain Model Describe Weak Polyelectrolyte Random Copolymers in Dilute Aqueous Solution?

Andi Xie, Panagiotis G. Georgiou, Jan Skov Pedersen, Steven P. Armes, and Anthony J. Ryan*

Cite This: https://doi.org/10.1021/acs.macromol.6c00697
Read Online

ABSTRACT: A series of weakly basic random copolymers composed of 2-(dimethylamino)ethyl methacrylate (DMA) and poly(ethylene glycol) methyl ether methacrylate (PEGMA) were synthesized to investigate the influence of charge on their solution behavior. The random comonomer distribution was confirmed via ^{1}H NMR spectroscopy by calculating reactivity ratios and monitoring reaction kinetics. Their pH-responsive behavior was characterized by acid–base titration and zeta potential analysis, revealing a direct correlation between degree of protonation and copolymer charge density. Dynamic light scattering (DLS), transmission electron microscopy (TEM), and small-angle X-ray scattering (SAXS) studies revealed acid-induced changes in coil size and conformation, driven by intrachain electrostatic repulsion. Fitting SAXS data to a wormlike chain model combined with a polymer reference interaction site model (WLC-PRISM) enabled quantification of key parameters such as Kuhn length, interaction strength, and effective interaction distance to investigate the backbone flexibility and charge interactions. Higher degree of protonation led to more rigid, expanded coils, while salt screening reduced electrostatic interactions and coil dimensions. Concentration-dependent structural analysis highlighted interchain repulsion in the dilute regime, and structure factor scaling agreed with prior polyelectrolyte studies. Gel Permeation Chromatography – Multi-Angle Laser Light Scattering (GPC-MALLS) confirmed charge-induced coil swelling across a range of molecular weights. In summary, a WLC-based framework, when combined with PRISM-type interaction terms, provides a consistent and physically meaningful description of chain conformation for this class of weakly charged random copolymers within the explored pH, ionic strength, and concentration ranges.

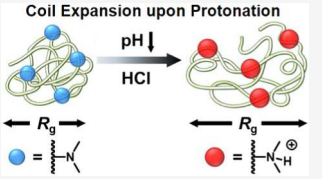

INTRODUCTION

Polyelectrolyte contain charged groups distributed along their backbones. Most linear polyelectrolytes are soluble in aqueous media: applications include water treatment,[1,2] drug delivery,[3,4] colloidal stabilization,[5,6] battery electrolytes,[7,8] and fundamental studies of various biological processes.[9,10] Nevertheless, our understanding of polyelectrolyte behavior remains incomplete.[11,12] Polyelectrolytes comprise both charged polymer chains and their associated counterions, which exhibit a rich and complex behavior driven by long-range electrostatic interactions (both intra- and interchain), short-range steric interactions and conformational entropy. As a result, the characterization and description of aqueous solutions of polyelectrolyte remains one of the most challenging topics within the field of soft matter.

The conformation of polyelectrolyte chains is determined by various complex interactions, including electrostatics,[13] hydrogen bonding,[14] polymer–solvent interactions,[15] excluded volume effects,[16–18] and covalent chain connectivity.[19] These complex interactions have substantial influence on chain flexibility. In general, polyelectrolyte backbones are less flexible than nonionic polymers owing to intrachain electrostatic repulsion, which leads to an expanded chain conformations in dilute solution.[13,20] Electrostatic interactions are typically dominant but the strength of such interactions may be modulated by adjusting salt concentration and pH. For example, the addition of salt screens long-range electrostatic repulsion, which results in chain contraction and reduced stiffness.[21,22] In addition, the solution pH affects the charge density of weak polyelectrolytes, thereby affecting their chain conformation.[23]

In dilute solution, the effective interactions between polyelectrolyte chains can be quantified by the second virial coefficient A_2 which provides a thermodynamic measure of interchain interactions.[24] For polyelectrolytes, A_2 is strongly influenced by long-range electrostatic interactions and therefore depends sensitively on charge density and ionic strength.[13] Classical descriptions based on screened Coulomb interactions predict an increase of the electrostatic contribution to A_2 with decreasing ionic strength, while charge regulation and counterion condensation can lead to deviations from ideal scaling behavior.[25–28] As such, analysis of A_2 offers a complementary perspective to single-chain conformational

Received: March 5, 2026
Revised: May 28, 2026
Accepted: June 26, 2026

parameters, linking intrachain electrostatics to interchain interactions in dilute polyelectrolyte solutions.

Understanding the structural characteristics of polyelectrolytes, particularly the relationship between chain conformations, charge distribution, and ionic strength, remains a complex challenge. Extensive investigations have been carried out over several decades using experimental methods,[29,30] theoretical models,[31,32] and computer simulations.[33,34] Small-angle scattering (SAS) techniques (neutron, X-ray or light) are commonly employed to study polymer chain conformation.[35−37] However, the relatively low X-ray scattering contrast of synthetic polyelectrolytes limits the data quality that can be obtained in such experiments.[38] Consequently, theoretical modeling has become an essential tool for investigating polyelectrolyte behavior in solution.

The worm-like chain (WLC) model, also referred to as the Kratky−Porod model, is widely used to describe the conformational behavior of semiflexible polymers in solution. However, in its classical form it is only applicable to stiff chains, for which the self-avoidance is neglected.[39] More recent derivations incorporate excluded-volume effects and are therefore applicable to semiflexible polymers in good solvents.[40,41] This model has been successfully applied to liquid crystalline polymers and conjugated systems.[42−44] For example, Murnen et al. investigated the chain conformations of synthetic polypeptoids comprising repeat units bearing various acidic group using small-angle neutron scattering (SANS) and found a reduction in the mean persistence length with increasing salt concentration.[45] The radius of gyration (R_g) was obtained from a Guinier fit to the data or calculated from the contour length (L) and Kuhn length (b) using the WLC model.[46,47] The WLC model also allows calculation of the end-to-end distance (R_{ee}), which can also be determined using double electron−electron resonance (DEER) spectroscopy.[48] These two parameters are essential for a comprehensive description of the chain conformation and aqueous solution behavior.[48]

In the WLC model, semiflexible chains adopt rigid rod-like conformations when the Kuhn length exceeds the contour length. In this case, the end-to-end distance is approximately equal to the copolymer contour length. This behavior is typically observed for semiflexible polymers with relatively low molecular weights. For longer chains, more flexible coil conformations are adopted with an intrinsic chain stiffness, resulting in the following equation that links R_{ee} and contour length using Kuhn length, which is mathematically double to persistence length (l_p):[49]

$$R_{ee}^2 = Lb\left[1 - \frac{b}{2L}(1 - e^{-2L/b})\right] \quad (1)$$

where the R_{ee}^2 is equivalent to $6R_g^2$ for a Gaussian copolymer coil as the chain length tends to infinity. Note that this expression neglects excluded volume effects.

Although the physical properties of synthetic weak polyelectrolytes have been extensively examined in aqueous solution, the influence of charge density on chain conformation is not well understood. Furthermore, there are relatively few studies that combine scattering techniques, structural analysis, and theoretical modeling.[30,45,50] However, a framework does exist, namely the works of Pedersen et al. employing of Monte Carlo simulations to explore the properties of worm-like chains with both excluded volume and screened Coulomb interactions in single and multichains systems.[17,40,50,51] Although such models were chosen to describe wormlike micelles in aqueous solutions, the length scales and other physical parameters are not far removed from those of synthetic polymers, suggesting that this model should be more widely applicable.[41,52]

Herein, the effect of varying the mean degree of protonation, polymer concentration, salt concentration, and copolymer composition on the chain conformation of hydrophilic cationic copolymer chains in aqueous solution was systematically investigated. The chains are weakly basic random copolymers with one of the repeat units bearing a hydrophilic polyethylene glycol (PEG) pendant group, which ensures water-solubility for the neutral (uncharged) chains. More specifically, a series of methacrylic random copolymers were synthesized via reversible addition−fragmentation chain transfer (RAFT) copolymerization of 2-(dimethylamino)ethyl methacrylate (DMA) with poly(ethylene glycol) methyl ether monomethacrylate (PEGMA) to produce a broad range of comonomer compositions with relatively narrow molecular weight distributions. In addition, analogous polydisperse polymers were synthesized via conventional free radical polymerization to explore whether our findings were also applicable to polydisperse polyelectrolytes.

The chain conformations of these weak cationic polyelectrolytes were characterized at varying degrees of protonation using small-angle X-ray scattering (SAXS) in relatively dilute aqueous solution to assess the influence of electrostatic interactions. Characterization of the uncharged copolymer coils was performed using the Gaussian chain model and the WLC model with excluded volume effects. Scattering data obtained for charged polymer chains were analyzed using (i) a particle structure factor for screened Coulomb interactions in the mean spherical approximation (MSA) and (ii) expressions similar to the polymer reference interaction site model (PRISM) derived from Monte Carlo simulations.[53−55] Such models provide satisfactory data fits over a wide q range for various copolymer concentrations and charge densities, which has rarely been done.[56]

RESULTS AND DISCUSSION

Synthesis and Characterization

A series of P(DMA-*stat*-PEGMA) copolymers of varying DMA content and molecular weight was synthesized in ethanol by RAFT copolymerization of DMA with PEGMA (see Scheme 1). CPDB and AIBN were used as the chain transfer agent and initiator, respectively. The [CPDB]/[AIBN] molar ratio was maintained at 4.0 for all copolymerizations to ensure efficient chain transfer between the propagating copolymer radicals.

Scheme 1. Synthesis of P(DMA-stat-PEGMA) Random Copolymers by RAFT Statistical Copolymerization of DMA with PEGMA in Ethanol, Using CPDB as the RAFT Agent and AIBN as the Initiator to Produce a Series of Water-Soluble Copolymers with Tunable Degrees of Protonation

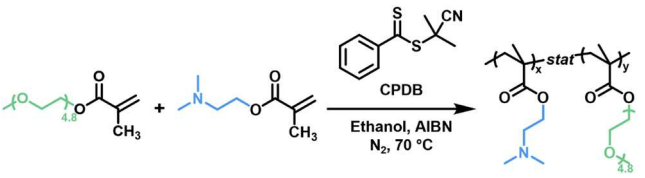

https://doi.org/10.1021/acs.macromol.6c00697
Macromolecules XXXX, XXX, XXX−XXX

Table 1. Summary of Comonomer Conversions, Compositions and Molecular Weights for Two Series of P(DMA-*Stat*-PEGMA) Random Copolymers

	^{1}H NMR[a]			DMF GPC[b]		Aqueous MALLS[c]	
Sample ID	DMA/mol %	Conversion	DP	M_w/g·mol^{-1}	$Đ$	$M_{w,abs}$/g·mol^{-1}	dn/dc/mL·g^{-1}
PD9010:150	10	63%	158	37,300	1.35	44,000	0.1235
PD8020:150	21	57%	143	34,100	1.35	41,300	0.1266
PD7030:150	29	59%	148	34,300	1.34	37,800	0.1294
PD6040:150	38	61%	153	31,800	1.33	36,900	0.1330

[a]Copolymer composition, conversion and DP were determined by ^{1}H NMR spectroscopy in $CDCl_3$. [b]Weight-average molecular weights (M_w) and dispersities ($Đ$) obtained by GPC analysis in DMF containing 0.02% w/w LiBr. [c]Absolute weight-average molecular weights ($M_{w,abs}$) and refractive index increment (dn/dc) values determined by MALLS and dRI analysis using aqueous eluent (pH 10) comprising 0.10 M $NaNO_3$, 0.02 M TEA, 0.05 M $NaHCO_3$, and 0.02% w/w NaN_3.

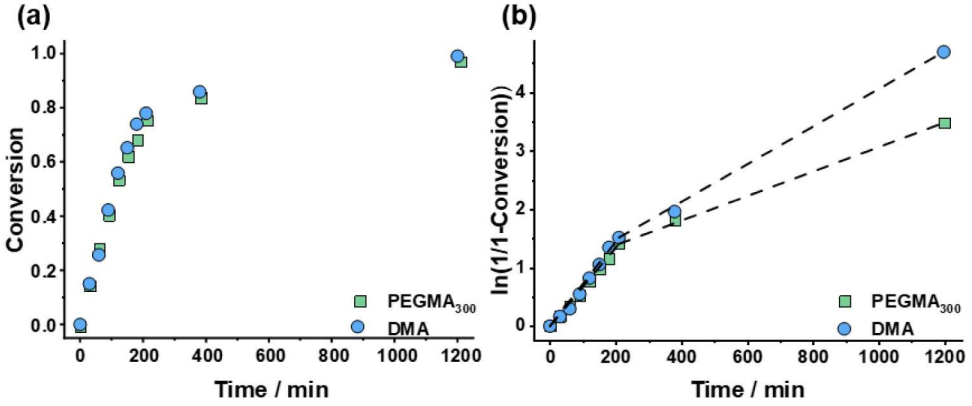

Figure 1. (a) Comonomer conversion as a function of time for the RAFT copolymerization of DMA with PEGMA (target DP = 250; target DMA content = 20 mol %) conducted at 70 °C, as determined by ^{1}H NMR spectroscopy. (b) Pseudo-first order kinetic plots.

RAFT polymerization enabled the synthesis of copolymers with relatively narrow molecular weight distributions and precisely controlled target molecular weights.[57] The resulting copolymers were purified by precipitation into *n*-hexane to remove any unreacted comonomer and then dried under vacuum at 40 °C. The residual comonomer content was less than 0.5% in all cases as determined by ^{1}H NMR spectroscopy. The final copolymers were viscous pink liquids, with the color resulting from the dithiobenzoate chain-ends. GPC analysis (DMF eluent) confirmed relatively narrow molecular weight distributions, with copolymer dispersities ($Đ$) ranging from 1.26 to 1.35. All copolymers had absolute weight-average molecular weights ($M_{w,abs}$) between 20 and 45 kDa, as determined using a MALLS instrument coupled to a differential refractometer (Table 1 and Figure S1).

The comonomer distribution critically affects copolymer structure and properties.[58] Despite aiming for statistical copolymers, reactivity differences often lead to sequence bias. In the present study, DMA and PEGMA were copolymerized at feed ratios ranging from 10:90 to 40:60 while ^{1}H NMR spectroscopy was used to confirm that overall copolymer compositions matched the initial feeds. Real-time ^{1}H NMR monitoring when using a 1:4 [DMA]:[PEGMA] comonomer feed indicated comparable rates of polymerization for each comonomer, with DMA reacting only slightly faster than PEGMA. More specifically, $k_{obs,DMA}$ = 0.0076 s^{-1} and $k_{obs,PEGMA}$ = 0.0067 s^{-1}, declining to 0.0033 s^{-1} and 0.0021 s^{-1} after 200 min (see Figure 1).

Comonomer reactivity ratios were determined using the extended Kelen–Tüdös method (Figure 2). This approach gave $r_{1,DMA}$ = 0.88 and $r_{2,PEGMA}$ = 0.83 (R^2 = 0.9913), suggesting a slight initial preference for DMA, which is offset at higher conversions. Hence the resulting P(DMA-*stat*-PEGMA) copolymers comprise a statistical distribution of DMA repeat units along each chain. Further detailed calculations are shown in Table S2.

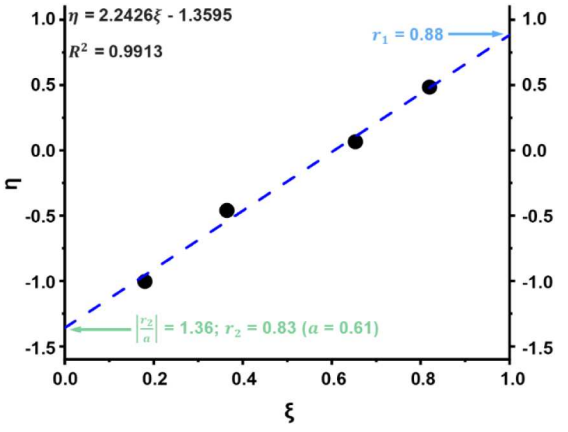

Figure 2. Corresponding comonomer reactivity ratio plot (α = 0.61), calculated using the Kelen-Tüdös method. The reactivity ratios were r_1,DMA = 0.88 and $r_{2,PEGMA}$ = 0.83, indicating comparable reactivities for these two methacrylic comonomers.

Higher conversions led to broader molecular weight distributions. After 20 h, DMF GPC showed a higher molecular weight shoulder peak (M_p = 40,500 g·mol^{-1}) in addition to the main peak (M_p = 22,700 g·mol^{-1}), which suggests some degree of chain termination via combination. In view of this, copolymerizations were quenched after 4 h to ensure low dispersities (see Figure 3).

https://doi.org/10.1021/acs.macromol.6c00697
Macromolecules XXXX, XXX, XXX−XXX

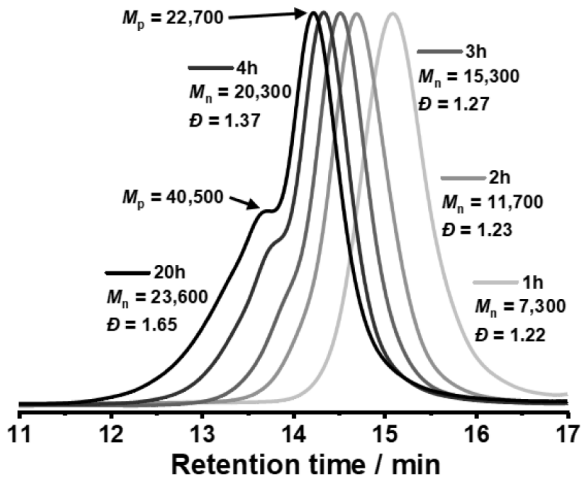

Figure 3. DMF GPC traces obtained during the RAFT copolymerization of DMA with PEGMA, showing the evolution of M_n and Đ overtime (target DP = 250; target DMA content = 20 mol %) conducted at 70 °C.

pH-Responsive Behavior in Aqueous Solution

The pH-responsive behavior of these copolymers and their corresponding chain conformations were systematically characterized using acid titration, DLS and zeta potential measurements. Acid titrations were conducted on aqueous copolymer solutions prepared using deionized water to examine the correlation between net acid addition, mean degree of protonation and solution pH. Each copolymer was dissolved in deionized water at 1.0% w/v, and the resulting solution was divided into two portions. These portions were titrated to pH 2 and pH 11 using 0.1 M HCl and KOH, respectively. Figure 4a presents typical titration curve obtained for a PD8020:150 statistical copolymer, where the *x*-axis represents the net amount of added HCl (positive values) or KOH (negative values), respectively. A buffer region was observed, indicating that the copolymer behaves as a weak base and is partially protonated within a specific pH range. At pH 9, the copolymer was fully deprotonated but its hydrophilic PEG units ensure that the neutral chains remain water-soluble. At pH 4.5, the DMA repeat units are fully protonated. Figure 4b displays the same titration curve as in Figure 4a, with the *x*-axis replaced by the mean degree of protonation (α) of the DMA units. The pK_a of the copolymer was determined to be between 6.9 and 7.0, which is slightly lower than that reported for PDMA homopolymer in dilute aqueous solution (pK_a = 7.6).[59]

DLS and TEM are commonly used for nanoparticle characterization. The former technique reports the hydrodynamic z-average diameter (D_h) for equivalent monodisperse noninteracting spheres.[60] TEM enables the nanoparticle morphology to be examined but this imaging technique suffers from relatively poor statistics and typically cannot resolve individual copolymer chains.[61] Scattering techniques also can be employed to investigate the nanoscale structure of polyelectrolytes. The resolution limit for MALLS (a.k.a. static light scattering, or SLS), is normally considered to be 10 nm,[62] whereas the shorter X-ray wavelength employed for SAXS allows smaller structures to be characterized. Accordingly, copolymers were characterized using DLS, TEM, SAXS, and MALLS.

It is well established that weak polyelectrolytes tend to adopt a more expanded conformation in solution compared to their neutral form owing to electrostatic repulsion between charged repeat units.[13,20] Moreover, increasing the degree of protonation should lead to larger copolymer coils. However, DLS analysis indicated a *reduction* in D_h with increasing acid concentration. Upon full protonation of the DMA repeat units, further addition of acid led to a slight increase in size (see Figure 5a). To investigate these unexpected observations, aqueous electrophoresis experiments were conducted. The zeta potential data indicated an isoelectric point at approximately pH 8, corresponding to the pH at which the zeta potential crosses zero (see Figure 5b); the copolymer chains possess no net charge at this condition, which corresponded to the maximum D_h. This behavior is attributed to concentration-dependent interchain interaction effects. In polyelectrolyte and charged copolymer systems, the apparent hydrodynamic radius obtained from DLS is known to be influenced by electrostatic and hydrodynamic interactions between chains. Increasing the degree of protonation reduces these interaction effects through enhanced electrostatic screening,[27] leading to an apparent decrease in D_h. Although intrachain electrostatic repulsion may contribute to conformational expansion, this effect is expected to be relatively small compared to the contribution from interaction-induced changes in the apparent hydrodynamic size.

It is perhaps worth emphasizing that DLS has inherent limitations in terms of resolution and reports a sphere-equivalent diameter, which limits its applicability to non-

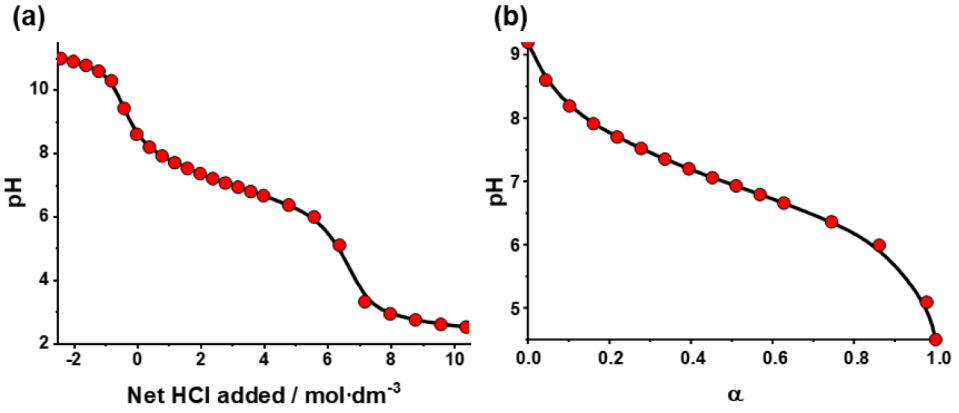

Figure 4. (a) Acid–base titration curve recorded for a 1.0% w/v aqueous solution of the PD8020:150 random copolymer. (b) Same titration data plotted against the mean degree of protonation, α.

https://doi.org/10.1021/acs.macromol.6c00697
Macromolecules XXXX, XXX, XXX−XXX

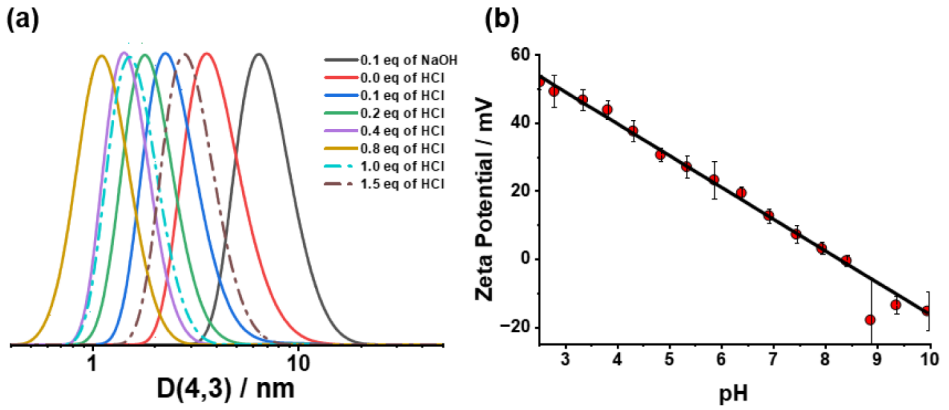

Figure 5. (a) Particle size distributions obtained by DLS at various acid addition conditions. (b) Zeta potential as a function of pH for a 0.5% w/w aqueous solution of a PD8020:150 copolymer.

spherical particles/aggregates.[63] In addition, the diffusion of charged particles in aqueous solution is highly sensitive to ionic strength, which complicates DLS measurements.[64] Consequently, interpreting the solution behavior of weak polyelectrolytes based solely on DLS data can be misleading. Complementary analytical techniques are essential for more reliable information.

TEM analysis revealed a clear morphological difference between the net neutral (~ pH 8) and fully protonated (~ pH 4) PD8020:150 copolymer chains. Relatively large, ill-defined dried aggregates were observed at pH 8 (Figure 6a), whereas

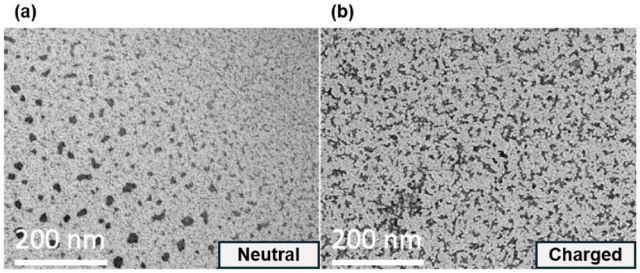

Figure 6. Representative TEM images recorded for a dilute aqueous solution of PD8020:150 copolymer chains: (a) net neutral (~ pH 8) and (b) fully protonated (~ pH 4).

the corresponding protonated copolymer chains formed smaller weakly nonisotropic structures (Figure 6b). To further investigate the chain conformation, a series of SAXS experiments were conducted.

SAXS Analysis

SAXS experiments were performed on aqueous copolymer solutions to obtain a deeper understanding of the effect of varying the cationic charge density on copolymer chain conformation and molecular ordering in solution. Accordingly, scattering data were recorded at various copolymer concentrations, salt concentrations, and solution pH.

SAXS samples were prepared by initially dissolving the copolymer in deionized water at a relatively high concentration of 5.0% w/w. A 0.1 M HCl solution was then added to protonate the DMA units, resulting in cationic copolymer chains. The [DMA]/[HCl] molar ratio was systematically varied from 0.1 to 2.0. The correlation between acid addition and the degree of protonation was examined by acid titration, as discussed above. The resulting solution was diluted with deionized water to prepare copolymer solutions at concentrations ranging from 0.1% to 1.5% w/w. For samples containing added salt, aqueous solutions of HCl and KCl were prepared at volume ratios of 2:1 and 1:1 to obtain solutions with two distinct [HCl]/[KCl] molar ratios. These solutions were added to the copolymer to both protonate the DMA units and introduce background salt. The presence of salt was expected to screen electrostatic interactions.[65] This preparation protocol was used for all SAXS samples.

Model Selection

As shown in Figure 7, the SAXS data recorded for 1.0% w/w aqueous solutions of PD8020:150 in either acidic solution ([HCl]/[DMA] = 1.0) or deionized water exhibit significant differences. The data obtained for the net neutral copolymer chains in water is consistent with that expected for semiflexible random coils in dilute solution. Within the Guinier regime, an

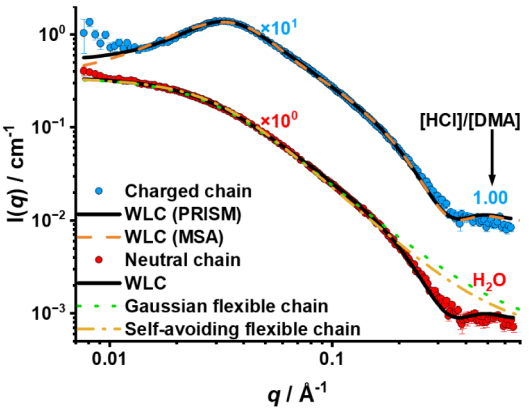

Figure 7. Synchrotron SAXS data recorded for 1.0% w/w aqueous solutions of PD8020:150 copolymer in its net neutral (red symbols) or charged (blue symbols) state. The red data set obtained for the neutral copolymer was fitted using three different models: a Gaussian chain model (dashed orange line), a self-avoiding flexible chain model (dotted green line), and a self-avoiding worm-like chain (WLC) model (solid black line). While all three models describe the low q region reasonably well, only the WLC model, which assumes a finite cross-section, provides a satisfactory fit across the whole q range. The charged copolymer (blue symbols) was fitted using the WLC model combined with an empirical structure factor derived from PRISM theory (black line) and the MSA repulsive structure factor (orange dashed line). In this case, both models account quite well for interchain electrostatic interactions.

https://doi.org/10.1021/acs.macromol.6c00697
Macromolecules XXXX, XXX, XXX−XXX

R_g of approximately 51 Å was estimated from a Guinier plot.[66] For copolymer chains lacking a well-defined surface, the scattering intensity I(q) follows a power-law decay at intermediate q (also known as the scaling region), such that $I(q) \sim q^{-p}$.[46] Data fitting yielded a power law exponent, p, of 2.2. This corresponds to a chain in a slightly poor, near-theta solvent, indicating a relatively contracted coil conformation.[67−69]

In acidic solution ([HCl]/[DMA] = 1.0), the SAXS data have a strong structure peak at low q, indicating significant interchain interactions.[46] Thus, the particle size cannot be estimated using the Guinier approximation. Instead, five scattering models were examined in turn to fit the SAXS data. These were (i) Gaussian flexible chains, (ii) self-avoiding flexible chains, (iii) self-avoiding worm-like chains (WLC), (iv) and, respectively, the same WLC with a repulsive structure factor in MSA, and (v) with a structure factor expressed by PRISM.[55,70]

For the net neutral copolymer chains, models (i), (ii) and (iii) (see Supporting Information for further details) each provided satisfactory data fits in the low q region. The Gaussian chain model neglects both local stiffness and electrostatic interactions.[71] Including excluded volume effects certainly improves the fit but fails to account for the finite cross-section of the chains.[72] This limitation explains the deviation of the fit from the data in the high q regime ($0.2 < q < 0.4$ Å^{-1}), which is influenced by the finite cylindrical cross-section of the copolymer chains. Owing to their methacrylic backbone, these copolymer chains possess restricted flexibility and exhibit rod-like character at short length scales. Hence, they are more accurately described as flexible cylinders, and their scattering profiles are best fitted using the self-avoiding WLC model, which includes a finite cross-section (see Equation S6).[39,51] This approach yielded a satisfactory fit to the SAXS data for the neutral copolymer. The contour length of the PD8020:150 copolymer in deionized water was calculated to be 378 Å, from the mean degree of polymerization (DP = 143) determined by ^{1}H NMR spectroscopy, assuming a projection length of 2.5 Å per repeat unit. The fitted cross-section radius, r, value was 10.2 Å, and the Kuhn length was estimated to be 35.1 Å. For completeness, copolymer dispersity was also taken into account. The absolute dispersity $Đ_{abs}$ was calculated using the NMR-derived M_n value and the weight-average molecular weight M_w obtained from MALLS, giving $Đ_{abs}$ = 1.1 (Equation S10). For comparison, DMF GPC analysis gave a somewhat higher $Đ$ of 1.30. The former value was used for model fitting via the Schulz-Zimm distribution, as described by Equation S9,[73−75] However, this value was held constant for SAXS analysis as it is determined independently.

For semiflexible polymers with comparable contour length to Kuhn length, the Rg was calculated to be 51.1 Å.[50] While the WLC model provides a satisfactory overall fit to the SAXS data, it does not account for the upturn observed at low q. This deviation is attributed to a minor population of aggregates, as previously suggested for similar hydrophilic copolymer systems.[76] The fitting therefore represents an effective description dominated by the single-chain contribution, although some uncertainty in the extracted parameters may arise from the low-q deviation.

For charged copolymer chains, an appropriate structure factor must be introduced to account for the electrostatic interactions. Common approaches for calculating the structure factor of solid spherical charged particles interacting with a screened Coulomb potential are based on the Hyper Netted Chain (HNC),[77] Rogers−Young closure (RY),[78] or the mean spherical approximation (MSA).[54] However, the HNC and RY models only provide numerical solutions for the structure factor, which limits their practical use. Instead, the MSA model is widely used for charged particles because it provides an analytical solution for the structure factor. Nevertheless, this model has various limitations when applied to polymer chains. First, it neglects the connectivity of the repeat units and chain flexibility. Second, it assumes that the particles are solid spheres of uniform diameter with the charges located at the surface, so any spatial inhomogeneity of the charge distribution is ignored. Thus, although MSA may be an appropriate simplified model for preliminary evaluation, it is not well-suited for the analysis of (semi)flexible coils or nonspherical particles.[54] In contrast, the polymer reference interaction site model (PRISM)[53,55,70] considers the topology, flexibility, and charge-regulated structural response of copolymer chains by combining the interchain and intrachain structural correlations, making it particularly suitable for the analysis of charged random coils.[53] Based on the Monte Carlo simulation,[50] the following expression has been suggested:[79]

$$I(q) = nM_c^2 \frac{P(q)P_{cs}(q)}{1 + vc(q)P(q)} \tag{2}$$

where n is the number density of the polymer coils, v describes the strength of the interaction, M_c is the scattering mass of a chain (equal to chain volume multiplied by excess scattering length density), $P(q)$ is the form factor for the backbone of the self-avoiding semiflexible polymer chains, $P_{cs}(q)$ is an appropriate cross-section form factor, and $c(q)$ is the Fourier transform of the direct correlation function describing the interaction between polymer coils. For polyelectrolytes, the empirical form:[79]

$$c(q) = \frac{\sin(qR_c)}{qR_c} e^{(-q^2\sigma^2)} \tag{3}$$

describes the simulations, where σ describes the fuzziness of the local ordering and R_c is the effective chain-to-chain interaction distance.

As shown in Figure 7, the quality of the fit provided by the MSA model is comparable to that obtained with the PRISM model. However, the various MSA parameters lack physical significance. Consequently, despite being empirical, the PRISM model is preferred because it provides a physically realistic scattering model for analyzing polyelectrolyte conformations due to its derivation from simulations. The contour length and cross-sectional cylinder radius were determined from the data fit for the net neutral copolymer and these two parameters were then kept fixed for the other fits. The contour length only depends on the mean degree of polymerization of the copolymer chains and hence should also remain constant regardless of the solution pH or salt concentration. The cross-sectional cylinder radius is related to the size of the PEG side-group. To fit copolymer chains with differing degrees of protonation, it is assumed that these PEG side groups are not affected by HCl or by the development of charge on the DMA repeat units. If this assumption is valid, then the cylinder radius must be independent of the degree of protonation of the copolymer chains. To analyze the charged copolymer chains, a

https://doi.org/10.1021/acs.macromol.6c00697
Macromolecules XXXX, XXX, XXX−XXX

sequential fitting strategy was used. Structural parameters obtained for the neutral system (contour length and effective cross-sectional radius) were assumed invariant upon protonation and fixed. The Kuhn length was taken as an initial estimate but allowed to vary to capture electrostatic stiffening. All PRISM interaction parameters (e.g., interaction strength and effective interaction distance) were treated as adjustable fitting parameters, enabling separation of intrinsic chain geometry from charge-dependent effects. For a [HCl]/[DMA] molar ratio of 1.0, the Kuhn length was 39.4 Å and the three parameters related to the direct correlation function were $\nu = 7$, $\sigma = 44$ Å and $R_c = 51$ Å, respectively. The term ν represents the strength of direct interactions between charges at different spatial scales (eqs 2 and 4). According to standard polymer theory, at low concentration,

$$\nu = 2M_w A_2 c \tag{4}$$

where A_2 is the second virial coefficient and c is the polymer concentration.[75]

Degree of Protonation and Salt Screening

After identifying the appropriate scattering model and fitting strategy, the SAXS data obtained for PD8020:150 at varying degrees of protonation were fitted to examine changes in the conformation adopted by this copolymer in its neutral form, fully protonated state, and charge-screened condition. Analysis of the variation in the Kuhn length and charge-related parameters revealed the relationship between the mean degree of protonation and the chain flexibility. The contour length determined from the neutral copolymer was assumed invariant upon protonation and fixed. The Kuhn length was fitted to capture changes in apparent chain stiffness, while interaction parameters (ν, σ, and R_c) were treated as adjustable to describe electrostatic-related effects. The SAXS data and corresponding fitting curves are shown in Figure 8 and the corresponding parameters calculated from the data fits are summarized in Table 2.

Inspecting Figure 8, the SAXS data recorded for this copolymer at various pH differ significantly. No obvious structure factor was observed in either deionized water or in the presence of excess acid, indicating that electrostatic interactions are either weak or negligible under such conditions. In deionized water, the near-neutral copolymer chains experience minimal electrostatic repulsion, resulting in a relatively compact conformation. In contrast, for excess HCl in acidic solution, the electrostatic repulsion between the fully protonated DMA repeat units is effectively screened owing to the relatively high ionic strength. This attenuates the otherwise strong interaction, thereby producing a relatively compact chain conformation. In addition, the neutral copolymer was fitted by assuming that there was no electrostatic interaction between neighboring chains, i.e., the interaction parameter, ν, was fixed at zero.

An additional layer of condensed counterions may surround the copolymer chains in the presence of excess acid.[80] This interaction is not fully captured by the WLC-PRISM model, resulting in a relatively large fitting deviations in low q region. Moreover, a low level of protonation of the DMA repeat units in deionized water results in a small electrostatic contribution to chain stiffness, such that the effective Kuhn length is slightly larger than that of the salt-screened copolymer. As the pH is decreased, the copolymer exhibits the expected polyelectrolyte response: the effective Kuhn length increases with the degree

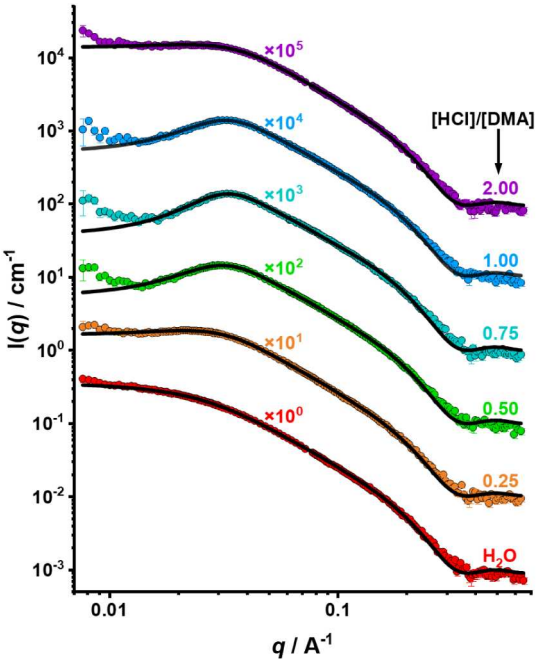

Figure 8. Synchrotron SAXS data recorded for 1.0% w/w aqueous solutions of PD8020:150 at various [HCl]/[DMA] molar ratios. All scattering data were fitted using the WLC-PRISM model. For clarity, curves are vertically shifted by an arbitrary factor, as indicated.

of protonation due to enhanced intrachain electrostatic repulsion.[81,82] This trend can be discussed within the Odijk-Skolnick-Fixman (OSF) framework,[18,82−84] in which the Kuhn length is written as

$$b = b_0 + b_{el} \tag{5}$$

where b is the Kuhn length, b_0 describes the contribution from intrinsic backbone stiffness and b_{el} is the contribution from the electrostatic interactions, $b_{el} = a\frac{Z_{eff}^2}{I}$. The parameter a is a prefactor that scales electrostatic term Z_{eff}^2/I to a physically reasonable magnitude. It can be estimated either from theoretical considerations or determined empirically. Under semiquantitative conditions, this approximation is considered acceptable.

In the present system, the observed increase in b with protonation is consistent with an increasing effective charge density Z_{eff}, while the comparatively large offset indicates that the b_0 term makes a dominant contribution under our experimental conditions. Notably, the pH-dependent trend in b broadly mirrors that in A_2, which is consistent with both quantities being sensitive to the strength of electrostatic repulsion, although their relative sensitivities differ.

Furthermore, three key parameters can be calculated by fitting the structure factor: the strength of direct interactions between charges at different spatial scales, ν, the ordering fuzziness σ, and the effective interaction distance R_c, as shown in Table 2. The ν parameter gradually increases at higher degrees of protonation, suggesting that electrostatic repulsion plays a major role in driving the change in copolymer conformation. Although a 1:1 [HCl]/[DMA] molar ratio matches the stoichiometry for full protonation, the DMA repeat units are almost fully charged at slightly lower ratios. The parameters σ and R_c are nearly of the same magnitude for polymers with a clear peak ([HCl]/[DMA] = 0.5, 0.75 and

https://doi.org/10.1021/acs.macromol.6c00697
Macromolecules XXXX, XXX, XXX−XXX

Table 2. Summary of SAXS Fitting Results Obtained for 1.0% W/W Aqueous Solutions of PD8020:150 at Various [HCl]/[DMA] Molar Ratios[a]

	Form Factor		Structure Factor		
[HCL]/[DMA]	b (Å)	R_g (Å)	ν	σ (Å)	R_c (Å)
0	35.1 ± 0.4	53.3	N/A	N/A	N/A
0.25	33.2 ± 0.7	52.1	1.2 ± 0.0	30.0 ± 2.7	79.8 ± 3.2
0.50	37.9 ± 0.7	54.9	6.1 ± 0.3	46.7 ± 6.5	45.9 ± 33.0
0.75	42.3 ± 0.9	57.2	10.1 ± 0.6	43.9 ± 3.1	64.3 ± 7.5
1.00	39.4 ± 0.8	55.7	7.0 ± 0.3	44.3 ± 4.9	50.6 ± 19.8
2.00	34.2 ± 0.7	52.8	1.6 ± 0.1	35.3 ± 37.1	15.1 ± 567.4

[a]All Scattering Data Were Fitted Using the WLC-PRISM Model. The Copolymer Contour Length (Defined by DP), Cross-Sectional Cylinder Radius and Dispersity Were Fixed at 378 Å and 10.2 Å and 1.1, Respectively. The Kuhn Length b was Fitted Using WLC Form Factor, While R_g was Calculated from the Fitted parameters.[50] Structure Factor Parameters ν, σ, and R_c Were Obtained from PRISM-Based Fitting.

1.0), where the strength of the interactions is larger than the thermal energy. This is because the characteristic interaction distance is determined by the copolymer concentration.

A similar set of experiments was conducted on PD6040:150, which is a copolymer of comparable molecular mass with a higher DMA content. Comparable SAXS data and corresponding fitting results were obtained for this copolymer (see Figure S2 and Table S3).

The above WLC-PRISM analysis assumes that the cross-sectional cylinder radius of the flexible copolymer chains remains consistent during protonation of the DMA repeat units. At around neutral pH, this scattering model provides a satisfactory fit to the experimental SAXS data. However, the SAXS data gradually deviate from the data fits at high q on addition of HCl. This is presumably related to the condensed counterions associated with the more strongly cationic chains, which increase the effective cylinder cross-sectional area and change the mean electron density, thereby affecting the X-ray contrast. This additional structural feature was not introduced to avoid overparameterization. A quantitative description of this layer of condensed counterions would require a more complex electric field-density coupling model.[85,86] In principle, contrast matching techniques using SANS with appropriate H_2O/D_2O mixtures might provide further structural insights.[87] However, such additional experiments are beyond the scope of the current study. Instead, the interaction between the PEG side-chains and cations was examined to assess the consistency of the cylinder cross-sectional area.

Contraction of copolymer chains in the presence of excess HCl was clearly observed. To investigate the effect of ionic strength on copolymer conformation and electrostatic interactions, SAXS experiments were performed at [KCl]/[HCl] molar ratios of 0.0, 1.0, and 2.0 while maintaining a constant [HCl]/[DMA] molar ratio and copolymer concentration to ensure the same mean degree of protonation. This strategy allows the effect of charge screening to be studied.

As shown in Figure 9, the structure peak gradually disappears at higher salt concentrations. The increased salt concentration results in a higher ionic strength, thereby reducing the electrostatic stiffening within the OSF framework. The observed decrease in Kuhn length is therefore consistent with suppression of long-range intrachain electrostatic repulsion, corresponding to a transition from a charge-dominated extended state to a more compact copolymer conformation.

The cylinder cross-sectional radius was treated as a fitting parameter to capture any influence by the anticipated layer of condensed counterions. The complex charge interactions

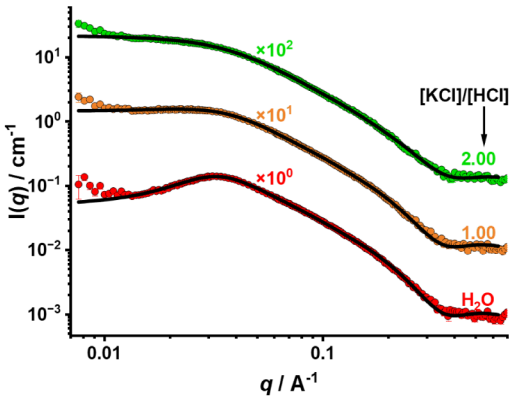

Figure 9. Synchrotron SAXS recorded for 1.0% w/w aqueous solutions of PD8020:150 at varying salt concentrations and a fixed [HCl]/[DMA] molar ratio = 1.0. All scattering data were fitted using the WLC-PRISM model. Salt concentrations are expressed in terms of the [KCl]/[HCl] molar ratio, as indicated for each curve. For clarity, curves are vertically shifted by arbitrary scaling factors, as indicated.

limited the fitting accuracy; nevertheless, added salt reduces the Kuhn length and the structure factor parameter ν, which is consistent with charge screening. These observations confirm that the ionic strength effectively modulates interchain interactions (Table 3).

The dimensionless fitting parameter ν obtained from the analysis is related to the second virial coefficient (A_2) via eq 4.[75] Using M_W = 41,300 g mol^{-1}, and c = 0.0101 g mL^{-1}, the extracted A_2 values fall in the range $10^{-3} - 10^{-2}$ mol ml g^{-2}, (see Table 4), which is comparable in magnitude to reported values.[55]

For weakly charged polyelectrolytes, the effective second virial coefficient contains an electrostatic contribution arising from screened Coulomb interactions between charged units.[13] In the dilute limit, the electrostatic contribution is predicted to scale with the inverse square of the Debye screening parameter (κ^{-2}), hence inversely with ionic strength (I).[83,84] A commonly used fitting form for second virial coefficient is[88]

$$A_2(I) = A_{2,0} + C\frac{f_{eff}^2 l_B}{\kappa^2} = A_{2,0} + C^*\frac{f_{eff}^2 l_B}{I} \quad (6)$$

where $A_{2,0}$ is the nonelectrostatic contribution, f_{eff} is the effective charge fraction and $C(C')$ is a factor that depends on chain properties. Deviations from the ideal I^{-1} scaling are potentially observed due to counterion condensation,[80,89] electrostatic stiffening[83,84] and many-body effects.

https://doi.org/10.1021/acs.macromol.6c00697
Macromolecules XXXX, XXX, XXX−XXX

Table 3. Summary of SAXS Data Fitting Results Obtained for a 1.0% W/W Aqueous Solution of PD8020:150 at Varying Salt Concentrations and a Fixed [HCl]/[DMA] Molar Ratio = 1.0[a]

	Form Factor		Structure Factor		
[KCL]/[DMA]	b (Å)	r (Å)	ν	σ (Å)	R_c (Å)
0.0	30.9 ± 1.2	9.5	6.1 ± 0.3	44.4 ± 3.3	55.1 ± 10.9
1.0	28.3 ± 0.5	9.5	1.3 ± 0.3	35.4 ± 0.5	10.0(fixed)
2.0	19.9 ± 1.5	8.7	0.2 ± 6.1	29.5 ± 3.8	10.0(fixed)

[a]All Scattering Data Were Fitted Using the WLC-PRISM Model. The Copolymer Contour Length and Dispersity Were Fixed at 378 Å and 1.1, Respectively. The Kuhn Length and Cylinder Radius Were Fitted in the WLC Form Factor. Structure Factor Parameters ν, σ, and R_c Were Obtained from PRISM-Based Fitting.

Table 4. Second Virial Coefficients A_2 Calculated from the Fitted Interaction Parameter ν at Different HCl/DMA Ratios and KCl/DMA (HCl/DMA was Fixed at 1.0) Ratio

[HCl]/[DMA]	M_w / g mol^{-1}	Conc./g mL^{-1}	ν	A_2 / ml mol g^{-2}
0.25	41,300	0.0101	1.2	0.00144
0.50			6.1	0.00733
0.75			10.1	0.01210
1.00			7	0.00841
2.00			1.6	0.00192
[KCl]/[DMA]	M_w / g mol^{-1}	Conc./g mL^{-1}	ν	A_2 / ml mol g^{-2}
0.00	41,300	0.0101	6.1	0.00733
1.00			1.3	0.00156
2.00			0.2	0.00024

To examine the role of electrostatic screening in the present system, the dependence of the extracted interaction parameter ν (and equivalently A_2) was analyzed using different definitions of ionic strength. When ionic strength was calculated solely from mobile small ions (Cl^- and excess H^+), the corresponding electrostatic scaling variable exhibited a pronounced dependence on the degree of protonation, closely following the experimental variation of ν. In contrast, inclusion of a formal macroion contribution to the ionic strength resulted in a much weaker dependence, see Figure 10. This comparison indicates that electrostatic screening is dominated by mobile small ions rather than by polymer charges themselves (and that $A_{2,0}$ is small), which is consistent with the assumptions underlying descriptions of the Debye–Hückel type and with the macroion nature of multiple chargers on polymer chains.[88,90]

It is noted that this analysis concerns the dilute-solution virial description of chain-to-chain interactions and although we observed a peak in the intensity, it should be distinguished from the semidilute regime, where interchain correlations also give rise to a characteristic polyelectrolyte peak in scattering experiments. The latter reflects correlation length physics rather than the second virial coefficient and is not directly addressed here.[56]

As discussed above, in addition to the A_2 value, which is directly correlated to the structure factor parameter ν, the Kuhn length is also closely connected to the electrostatic repulsion, though their sensitivities are not identical. Figure 11 therefore compares the experimentally extracted b values with the trend inferred as a function of degree of protonation.

The theoretical variation of b was estimated using a semiquantitative OSF-type expression as stated by eq 5 above. The Z_{eff}^2/I was scaled by an empirical prefactor a to bring the calculated variation into the experimentally range. This approach is not intended as a parameter-unique fit, but rather to illustrate that the observed trend is consistent with an electrostatic stiffening contribution that scales with Z_{eff}^2/I.

Figure 11 illustrates the response of b to two electrostatic perturbations. Increasing the degree of protonation leads to an

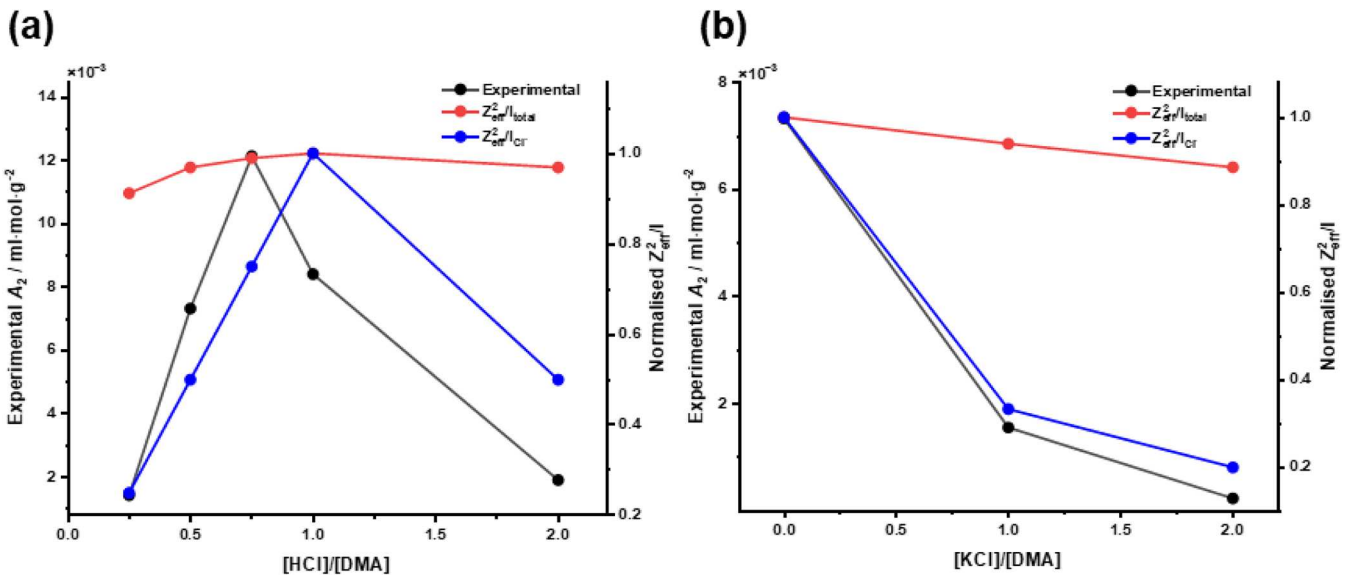

Figure 10. Experimental second virial coefficient A_2 and scaled Z_{eff}^2/I calculated using total ionic strength and small-ion (Cl^-) ionic strength as a function of HCl/DMA ratio (a) and of KCl/DMA (where HCl/DMA ratio was fixed at 1.0) ratio (b).

https://doi.org/10.1021/acs.macromol.6c00697
Macromolecules XXXX, XXX, XXX−XXX

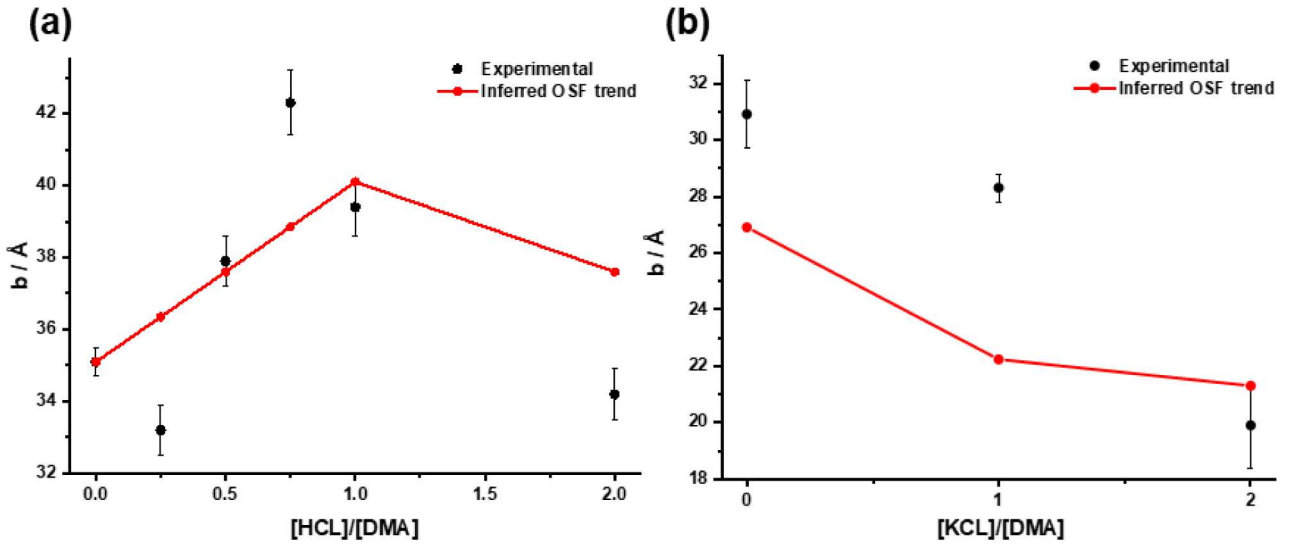

Figure 11. Variation of the experimentally determined b under two electrostatic perturbations. (a) dependence on degree of protonation; (b) dependence on added salt concentration.

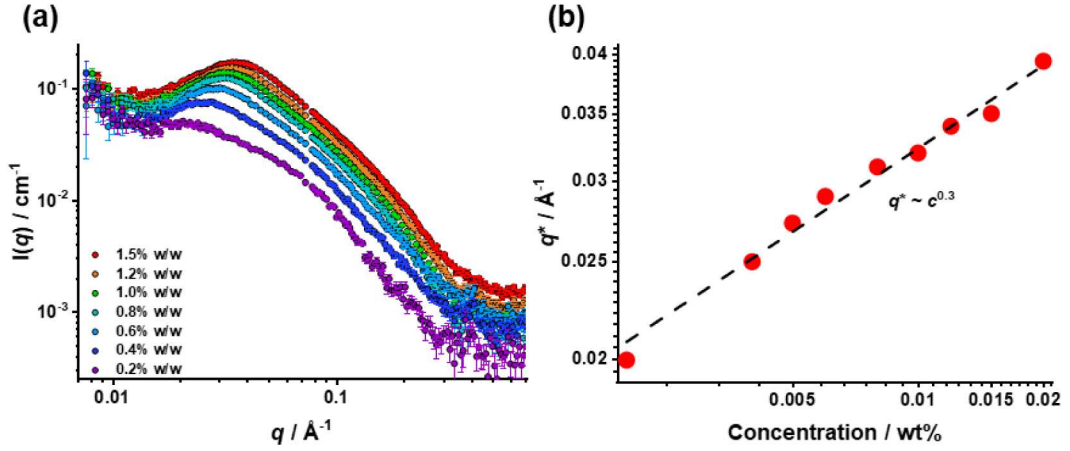

Figure 12. (a) Synchrotron SAXS recorded for a series of aqueous solutions of PD8020:150 at various copolymer concentrations and a fixed [HCl]/[DMA] molar ratio = 1.0. Copolymer concentrations are indicated in the Figure. Data are presented without vertical shifting to illustrate the concentration-dependent shift in the structure peak. (b) Copolymer concentration dependence of the structure factor peak position q^*. The dashed line represents a power law fit to the data, indicating that q^* scales with concentration as $c^{0.3}$.

increase in the extracted values, consistent with enhanced electrostatic stiffening. In contrast, added salt induces a systematic decrease, reflecting electrostatic screening. The opposite trends support an OSF-type interpretation in which the electrostatic contribution scales with Z_{eff}^2/I.

Effect of Copolymer Concentration

The copolymer concentration significantly affects the interchain and intrachain interactions, especially during the transition from the dilute to semidilute regime. This boundary is defined by the critical overlap concentration, c^*, above which the copolymer chains begin to interact with each other.[49] The value of c^* is given by

$$c^* = \frac{3M_w}{4\pi N_A R_g^3} \quad (7)$$

where N_A is Avogadro's constant. For typical values, in the present work, R_g = 50 Å, M_w = 43,100 g mol^{-1}, hence c^* = 0.14 g mL^{-1}.

However, the applicability of this approach for the analysis of polyelectrolytes in aqueous solution is controversial:[91−93] increasing the copolymer charge density introduces long-range electrostatic repulsion, so cationic chains may exhibit electrostatic interchain interactions at copolymer concentrations much lower than c^*.

SAXS measurements were performed at seven copolymer concentrations (0.2, 0.4, 0.6, 0.8, 1.0, 1.2 and 1.5% w/w) at a fixed full degree of protonation. The copolymer concentration was treated as the only variable to evaluate its effect on the chain conformation. As shown in Figure 12a, the X-ray scattering intensity and the structure peak are both reduced at lower copolymer concentration. However, a weak structure factor was still discernible even at 0.2% w/w, indicating electrostatic repulsion between neighboring cationic copolymer chains.

Inspecting Figure 12b, the structure peak position q^* is clearly dependent on the copolymer concentration. A plot of q^* versus copolymer concentration, c, reveals a power law relationship with an exponent close to 0.3, as expected for a

https://doi.org/10.1021/acs.macromol.6c00697
Macromolecules XXXX, XXX, XXX−XXX

Table 5. Summary of SAXS Data Fits Obtained for Aqueous Solutions of PD8020:150 at a Fixed [HCl]/[DMA] Molar Ratio = 1.0 and Variable Copolymer Concentrations[a]

	Form Factor		Structure Factor		
Conc./% w/w	b (Å)	r (Å)	ν	σ (Å)	R_c (Å)
1.5	23.4 ± 1.2	8.6	5.5 ± 0.3	38.3 ± 2.2	54.5 ± 6.7
1.2	25.3 ± 1.2	8.9	5.9 ± 0.3	41.8 ± 2.4	59.2 ± 6.7
1.0	29.1 ± 1.2	9.4	5.8 ± 0.3	43.4 ± 3.3	60.2 ± 9.4
0.8	30.0 ± 1.5	9.7	5.8 ± 0.2	52.4 ± 0.7	10.0(fixed)
0.6	19.9 ± 0.9	9.0	5.4 ± 0.5	65.8 ± 1.9	10.0(fixed)
0.4	15.7 ± 0.5	9.4	3.2 ± 0.5	75.8 ± 3.4	10.0(fixed)
0.2	27.3 ± 9.5	12.5	1.1 ± 0.4	12.8 ± 6.2	10.0(fixed)

[a]All Scattering Data Were Fitted Using the WLC-PRISM Model. The Copolymer Contour Length and Dispersity Were Fixed at 378 Å and 1.1, Respectively. The Kuhn Length and Cylinder Radius Were Fitted in the WLC Form Factor. Structure Factor Parameters ν, σ and R_c Were Obtained from PRISM-Based Fitting.

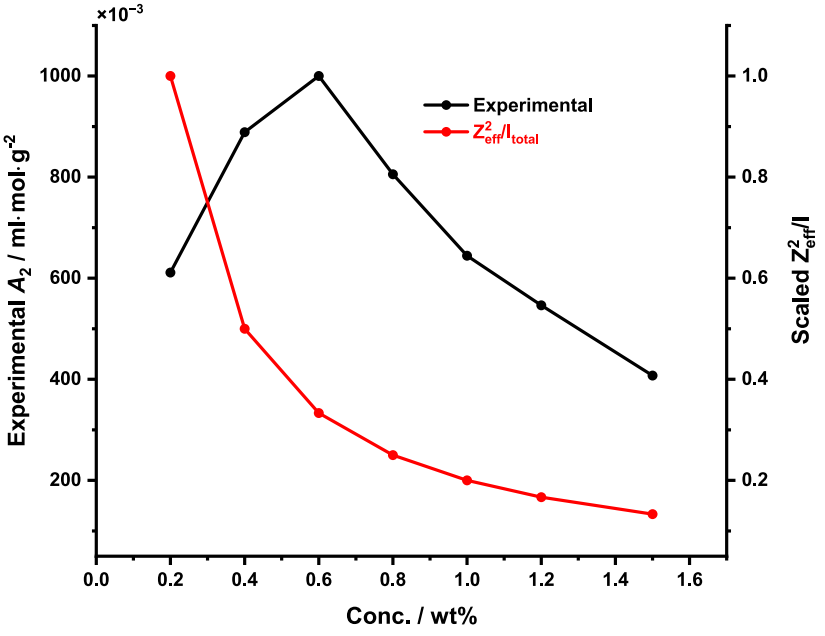

Figure 13. Concentration dependence of the experimental A_2, together with the scaled electrostatic term Z_{eff}^2/I expected from OSF theory.[75].

polyelectrolyte in dilute aqueous solution below c^*.[20,26] In contrast, the scaling relationship switches to $c^{0.5}$ above c^*.[94] Despite the presence of a structure peak, this suggests that the copolymer chains do not overlap or form entanglements, hence any change in conformation is primarily governed by long-range electrostatic repulsion. This agrees with the estimate of c^* for typical parameter values. To assess the effect of copolymer concentration on chain conformation and inter-chain interactions, these SAXS data were fitted using the WLC-PRISM model at a fixed degree of protonation of the DMA repeat units. At lower copolymer concentration, the copolymer chains expanded, as judged by the increase in Kuhn length, which indicates reduced chain flexibility. This is attributed to greater separation between isolated copolymer chains, rather than any variation in their charge density. Given the relatively low X-ray scattering contrast between the copolymer chains and water, the corresponding data fits should be interpreted with caution. A summary of the fitting results is presented in Table 5.

As shown in Figure 13, the experimentally determined A_2 parameter follows the same decreasing trend as the normalized Z_{eff}^2/I term above intermediate concentrations, as expected from OSF theory. At the lowest concentrations ($\lesssim$ 0.4 wt %), the extracted values exhibit larger scatter and deviate from the simple OSF trend. This regime is characterized by reduced scattering contrast and stronger parameter correlations in the fitting procedure. At higher concentrations (>0.5 wt %), however, a clear systematic trend emerges: the decrease in A_2 closely follows the reduction in the normalized Z_{eff}^2/I term. This behavior is consistent with an OSF-type electrostatic contribution to chain stiffness. The sizable offset indicates that the intrinsic Kuhn length b_0 dominates the absolute magnitude, while the electrostatic term primarily governs the observed concentration dependence in the semidilute regime.

The deviation at the lowest concentrations may reflect additional screening contributions not captured in the simple OSF description. In particular, residual counterions, macro-ion effects, or incomplete removal of low-molecular-weight species could contribute to the effective ionic strength at very low polymer concentrations. Such effects would modify the effective screening length and lead to departures from the ideal I^{-1} scaling.

For polyelectrolyte solutions with known concentrations, Plazzotta et al. proposed an alternative method to determine

https://doi.org/10.1021/acs.macromol.6c00697
Macromolecules XXXX, XXX, XXX−XXX

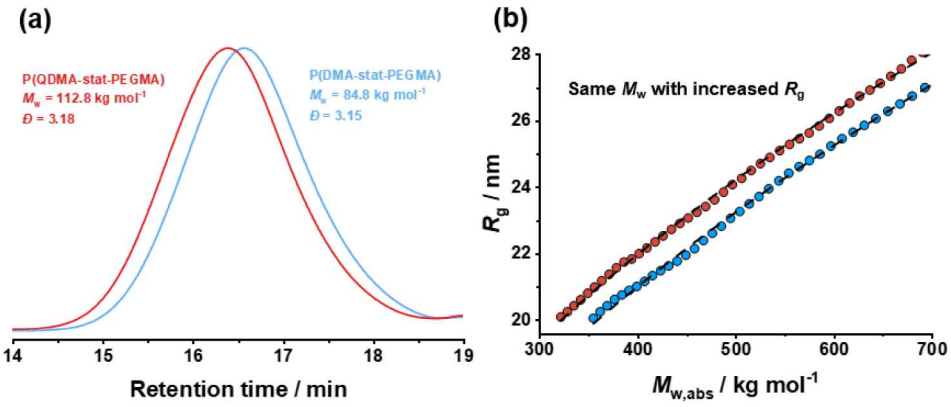

Figure 14. (a) Molecular weight distributions recorded for the polydisperse precursor copolymer prepared by conventional free radical copolymerization and its quaternized analogue. (b) $M_{w,abs}$ vs R_g plot obtained for the nonprotonated precursor FRP copolymer and its cationic quaternized analogue in aqueous eluent at pH 10 using GPC-MALLS with PMMA standards.

the molecular weight using SAXS, in which the M_n is correlated with q^*.[95] This approach features simple data analysis and is independent of the polymer's chemical structure. It has already been applied to polymers with diverse architectures and chemical compositions.[95] The calculation follows eq 8:

$$M_n = \frac{C_w N_A (2\sqrt{2}\pi/q^*)^3}{4} \quad (8)$$

where C_w is the mass concentration of the polyelectrolyte. It is important to note that this relationship requires sufficient contrast between the sample and solvent, polymer concentrations well below the c^*, and the sample must be charged. By extracting q^* values from the concentration series of SAXS data and calculating the C_W-q^* relationship, the M_n of the PD8020:150 sample was determined to be 34,500 ± 1,600 g·mol^{-1} (corresponding to M_w = 38,000 ± 1,800 g·mol^{-1} with $Đ$ = 1.1). This result is comparable to the M_w obtained from MALLS (41,300 g·mol^{-1}) measurements and falls within a 10% deviation.[95]

Quaternization of P(DMA-*Stat*-PEGMA) and Characterization of Chain Dimensions

To investigate polyelectrolyte behavior over a broader molecular weight range, a polydisperse random copolymer, denoted P(DMA$_{0.2}$-*stat*-PEGMA$_{0.8}$), was synthesized via free radical copolymerization. This copolymer exhibited a relatively broad molecular weight distribution that ranging from a few thousand to several million g·mol^{-1}. The pendant tertiary amine units were subsequently quaternized to form quaternary ammonium groups (denoted as P(QDMA$_{0.2}$-*stat*-PEGMA$_{0.8}$)), thereby imparting permanent cationic charge that is independent of solution pH. Both P(DMA$_{0.2}$-*stat*-PEGMA$_{0.8}$) and P(QDMA$_{0.2}$-*stat*-PEGMA$_{0.8}$) were analyzed by aqueous GPC-MALLS. An aqueous eluent was selected for this comparison because the quaternized copolymer proved to be insoluble in DMF.

Figure 14a depicts the aqueous GPC curves for each copolymer. The M_w and $Đ$ for the free radical polymerized copolymer were 84.8 kg·mol^{-1} and 3.15, respectively. As the GPC analysis provides relative molecular weight values based on PMMA calibration standards, the absolute value of the dispersity should be interpreted with caution. Quaternization of the precursor resulted in an increase in its apparent M_w, while the dispersity remained essentially unchanged. It should be noted that this M_w value is relative, as calibration was performed using poly(methyl methacrylate) standards.

A MALLS detector was coupled to the aqueous GPC instrument, and a refractive index detector was employed to determine the copolymer concentration based on the known differential refractive index increment (dn/dc) for each sample. For polyelectrolytes, uneven distribution of ions between the polymer coil and bulk solution can lead to a difference in chemical potential, which is referred as the Donnan effect. This effect may affect the measured dn/dc values and consequently the accuracy of the molecular weight.[96] In the present work, measurements were conducted in a pH 10 eluent with ionic strength significantly higher than the copolymer concentration (and chargeable unit in the polymer). Under these conditions, electrostatic interactions are strongly screened and the influence of ion partitioning on dn/dc is expected to be minimal, as reported in previous studies.[97−99] Therefore, the absence of dialysis is not expected to significantly affect the accuracy of the molecular weight determination. The dn/dc values were measured for four higher molecular weight copolymers at pH 10 eluent and increased with higher DMA content. Although PDMA homopolymer is not water-soluble at pH 10, extrapolation yielded a dn/dc of 0.172 mL·g^{-1} for this homopolymer under such conditions, which is comparable with values previously reported in acidic aqueous solution.[100] (Figure S3)

GPC analysis involves fractionation based on hydrodynamic volume, with long chains eluting prior to short chains. Hence the MALLS detector can simultaneously and continuously detect the M_w and R_g. Given the relatively long laser wavelength (650 nm) and the poor sensitivity of MALLS for the analysis of dilute copolymer solutions (<0.001 g·dm^{-3}), R_g values below 20 nm are unreliable. Figure 14b shows R_g as a function of M_w for P(DMA-*stat*-PEGMA) and P(QDMA-*stat*-PEGMA) at pH 10, with $M_{w,abs}$ values of less than 700 kg·mol^{-1} and R_g values greater than 20 nm. A $R_g \sim M_w^{\nu}$ scaling relationship was observed, where the Flory exponent ν = 0.45 is related to the solvent quality and the scaling of polymer size,[67] hence the inherent flexibility of the copolymer chain. According to the polymer physics literature, unperturbed chains that adopt a flexible random walk scale as $R_g \sim M_w^{0.5}$,[68,101,102] which corresponds to a typical Gaussian coil under θ-conditions. In contrast, $R_g \sim M_w^{0.588}$ for flexible chains dissolved in a good solvent that adopt a self-avoiding random

https://doi.org/10.1021/acs.macromol.6c00697
Macromolecules XXXX, XXX, XXX−XXX

walk,[69,101,103] while $R_g \sim M_w^{0.33}$ is characteristic behavior for collapsed coils in a poor solvent.[104] This parameter is indirectly defined by the exponent appearing in Equation S3 of the scattering function used to describe the SAXS data shown in Figure 7. The lower ν value of 0.45 indicated by MALLS analysis compared to $\nu = 0.60$ from SAXS for the neutral chains is attributed to the reduced solvation of the copolymer chains in the presence of added salt.[105] However, this is consistent with random coils over the whole measurement range accessible by MALLS, since the chains are nonprotonated at pH 10 (GPC eluent) so electrostatic interactions are screened and the solution structure factor is minimized, see Figure 10. Hence the self-avoiding chain model is applicable for both charged and neutral copolymer chains with a sufficiently long contour length under such conditions. The presence of PEG side chains ensures good solvent conditions. Under the experimental salt conditions, electrostatic interactions are sufficiently screened such that the conformational behavior of both neutral and charged copolymers can be reasonably described by the worm-like chain (WLC) model including excluded volume within the probed length scales.

A calculation using eq 1 based on the data set shown in Figure 14 gives $b = 39.8$ Å for the neutral and 43.4 Å for the quaternized random copolymers, respectively. The Kuhn length derived from MALLS are slightly larger than those obtained from SAXS. This difference is expected given the distinct experimental conditions (e.g., solvent composition, ionic strength and concentration) and the different analysis approaches (calculation in MALLS versus direct form factor fitting in SAXS). Therefore, quantitative agreement between the two techniques is not anticipated. Instead, consistency in the order of magnitude and the observed trend. An increase in chain stiffness upon charging should be considered meaningful. This level of agreement supports the physical interpretation of charge-induced chain expansion and stiffening, while not implying equivalence between the absolute values of persistence length obtained by the two methods Table 6.

Table 6. Comparison of Kuhn Lengths

SAXS (PD8020:150)		MALLS (PD8020:FRP)	
b (Å) Neutral	b (Å) Charged	b (Å) Neutral	b (Å) Charged
35.1	42.3	39.8	43.4

Interactions Between Poly(ethylene glycol) and Salt

In the above discussion, it was implicitly assumed that the PEG side-chains served only to enhance the aqueous solubility of the copolymer and that this nonionic component did not interact with either salt or acid. However, several studies suggest that PEG can interact with various anions and cations.[106−108] For example, Cao et al. reported that PEG homopolymer becomes protonated below pH 9.[107] Moreover, Rogers et al. found that longer PEG chains interacted more strongly with thiocyanate anion (SCN^-).[106] Similarly, Maltesh and Somasundaran found that various cations influence the conformation of PEG chains.[108] In principle, such ions may also affect the copolymer conformation at various salt concentrations and solution pH. Demonstrating that these effects are negligible for the present P(DMA-*stat*-PEGMA) system is important for validation of the WLC-PRISM model. Accordingly, a P(PEGMA) homopolymer was synthesized for SAXS analysis under identical solution conditions to investigate whether the PEG side-chains significantly influence the copolymer chain conformation. The SAXS data recorded for this P(PEGMA) homopolymer dissolved in deionized water or in the presence of 6.0 mM HCl are essentially identical, confirming that its chain conformation is independent of the solution pH (Figure 15). Refining the flexible

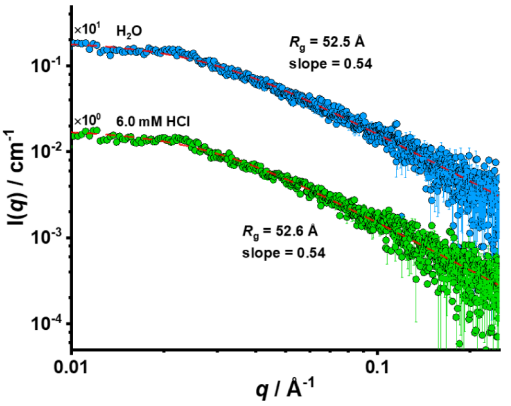

Figure 15. SAXS data recorded for 1.0% w/w aqueous solutions of P(PEGMA) homopolymer random coils using a Xeuss 2.0 instrument. The flexible polymer chain model (which accounts for excluded volume) was fitted to determine the mean R_g for the random coils formed by this neutral homopolymer in deionized water (blue data) and in 6 mM HCl aqueous solution (green data).

polymer model to account for the effect of excluded volume, the R_g and power law slope were calculated to be 52.5 Å and 0.54 in deionized water and 52.6 Å and 0.54 in the presence of 6.0 mM HCl, respectively. Thus, notwithstanding their role in diluting the cationic charge density, PEGMA repeat units act solely as a passive nonionic hydrophilic component when studying the conformation of the random copolymer polyelectrolytes reported herein.

CONCLUSIONS

A series of weakly basic P(DMA-*stat*-PEGMA) random copolymers was employed as a model system for investigating the effect of varying the charge density on the chain flexibility of polyelectrolyte chains. The random architecture of the copolymer chains was confirmed by determining comonomer reactivity ratios by ^{1}H NMR spectroscopy. The pH-responsive behavior was quantified using acid−base titration and zeta potential measurements, establishing a direct relationship between the degree of protonation and the resulting charge density along the copolymer chains. DLS and TEM studies indicated subtle changes in size and chain conformation on addition of acid, revealing the role of electrostatic repulsion on the solution behavior of these random copolymers. SAXS analysis provided detailed insight into the various chain conformations adopted by such neutral/charged copolymers and the self-assembly of the copolymer chains in solution. Introducing a WLC-PRISM model enabled calculation of key structural parameters, including the mean Kuhn length, interchain interaction strength, interaction fuzziness, and the effective interaction distance.

At around neutral pH, the copolymer chains adopt a relatively compact coil conformation, which expands at low pH due to intrachain electrostatic repulsion as the cationic charge density per chain builds up. Salt screening experiments indicated that electrostatic interactions are significantly

https://doi.org/10.1021/acs.macromol.6c00697
Macromolecules XXXX, XXX, XXX−XXX

attenuated at high ionic strength, resulting in a shorter Kuhn length and smaller, more compact coils. Systematic variation of the copolymer concentration also suggested the influence of interchain repulsion on coil conformation in the dilute regime. The scaling behavior of the position of the structure peak with copolymer concentration was consistent with prior studies of aqueous solutions of polyelectrolytes.[20,26] GPC-MALLS measurements were conducted to examine the molecular weight dependence for the coil size. Comparison between the weakly cationic P(DMA-*stat*-PEGMA) precursor and its permanently charged analogue, P(QDMA-*stat*-PEGMA), revealed a consistent trend of charged coil expansion across the entire molecular weight range, suggesting the generality of charge-induced swelling for such systems.

Overall, this study confirms that the chain conformation of such weakly basic random copolymers is governed by charge density, ionic strength and copolymer concentration. The WLC-based framework combined with a PRISM interaction term provides a consistent and physically meaningful description of chain conformation under the stated aqueous solution conditions, enabling accurate quantification of chain stiffness and electrostatic interactions. The intrinsic chain stiffness was quantified by the underlying WLC model, while charge interactions must be considered to capture electrostatic contributions. This combined approach offers a practical basis for interpreting scattering data acquired for weak polyelectrolyte random copolymers in aqueous solution.

■ ASSOCIATED CONTENT

Supporting Information

The Supporting Information is available free of charge at https://pubs.acs.org/doi/10.1021/acs.macromol.6c00697.

Experimental and Instrumental sections; additional Summary table of reagent quantities required in the synthesis of the random copolymers; MALLS plots obtained using the Zimm formalism for light scattering data collected for eight P(DMA_x-stat-$PEGMA_y$) random copolymers dissolved in a pH 10 eluent; Summary table of data and calculated parameters during Kelen-Tüdös calculation; SAXS data and fitting for PD6040:150 copolymer; scattering models used for SAXS analysis; representative differential refractive index data for a PD9010:150 random copolymer dissolved in pH 10 GPC buffer are available in the Supporting Information (PDF)

■ AUTHOR INFORMATION

Corresponding Author

Anthony J. Ryan − *Department of Chemistry, University of Sheffield, Sheffield, South Yorkshire S3 7HF, U.K.;* orcid.org/0000-0001-7737-0526; Email: a.ryan@sheffield.ac.uk

Authors

Andi Xie − *Department of Chemistry, University of Sheffield, Sheffield, South Yorkshire S3 7HF, U.K.*

Panagiotis G. Georgiou − *Department of Chemistry, University of Sheffield, Sheffield, South Yorkshire S3 7HF, U.K.;* orcid.org/0000-0001-8968-1057

Jan Skov Pedersen − *Department of Chemistry and Interdisciplinary Nanoscience Center (iNANO), Aarhus University, Aarhus C 8000, Denmark;* orcid.org/0000-0002-7768-0206

Steven P. Armes − *Department of Chemistry, University of Sheffield, Sheffield, South Yorkshire S3 7HF, U.K.;* orcid.org/0000-0002-8289-6351

Complete contact information is available at: https://pubs.acs.org/10.1021/acs.macromol.6c00697

Author Contributions

This work was conceived during a bike ride by A.J.R. and J.S.P. following a question raised during the Bombannes 2022, 15th European Summer School on "Scattering Methods Applied to Soft Condensed Matter". The experimental work was performed by A.X., with S.P.A. supervising the copolymer selection and synthesis, A.J.R. and J.S.P. guiding the SAXS modeling. TEM images were collected by P.G.G. The first draft was written by A.X. All authors discussed the results and commented on the manuscript.

Notes

The authors declare no competing financial interest.

■ ACKNOWLEDGMENTS

M. A. H. Farmer, M. Allen, P. Chohan, J. J. S. Tyler and M. A. Newell are acknowledged for collecting the Synchrotron SAXS data, O. O. Mykhaylyk is thanked for useful discussion and suggestions. Diamond Light Source and ESRF are thanked for providing beamtime.

■ REFERENCES

(1) Bolto, B.; Gregory, J. Organic Polyelectrolytes in Water Treatment. *Water Res.* **2007**, *41* (11), 2301−2324.

(2) Chen, M.; Xu, R.; Wu, Y.; Xiong, J.; Keleş, S. Z.; Hankins, N. P. Application of Polyelectrolytes for Contaminant Removal and Recovery during Water and Wastewater Treatment: A Critical Review. *J. Water Proc. Eng.* **2024**, *64*, 105528.

(3) Gradzielski, M. Polyelectrolyte−Surfactant Complexes As a Formulation Tool for Drug Delivery. *Langmuir* **2022**, *38* (44), 13330−13343.

(4) Yang, Q.; Wang, S.; Fan, P.; Wang, L.; Di, Y.; Lin, K.; Xiao, F.-S. PH-Responsive Carrier System Based on Carboxylic Acid Modified Mesoporous Silica and Polyelectrolyte for Drug Delivery. *Chem. Mater.* **2005**, *17* (24), 5999−6003.

(5) Semsarilar, M.; Ladmiral, V.; Blanazs, A.; Armes, S. P. Anionic Polyelectrolyte-Stabilized Nanoparticles via RAFT Aqueous Dispersion Polymerization. *Langmuir* **2012**, *28* (1), 914−922.

(6) Pefferkorn, E. The Role of Polyelectrolytes in the Stabilisation and Destabilisation of Colloids. *Adv. Colloid Interface Sci.* **1995**, *56*, 33−104.

(7) Tiyapiboonchaiya, C.; Pringle, J. M.; Sun, J.; Byrne, N.; Howlett, P. C.; MacFarlane, D. R.; Forsyth, M. The Zwitterion Effect in High-Conductivity Polyelectrolyte Materials. *Nat. Mater.* **2004**, *3* (1), 29−32.

(8) Hu, X.; Dong, H.; Gao, N.; Wang, T.; He, H.; Gao, X.; Dai, Y.; Liu, Y.; Brett, D. J. L.; Parkin, I. P.; et al. Self-Assembled Polyelectrolytes with Ion-Separation Accelerating Channels for Highly Stable Zn-Ion Batteries. *Nat. Commun.* **2025**, *16* (1), 2316.

(9) Rubinstein, M.; Papoian, G. A. Polyelectrolytes in Biology and Soft Matter. *Soft Matter* **2012**, *8* (36), 9265−9267.

(10) Katchalsky, A. Polyelectrolytes and Their Biological Interactions. *Biophys. J.* **1964**, *4* (1), 9−41.

(11) Lopez, G. C.; Matsumoto, A.; Shen, A. Q. Dilute Polyelectrolyte Solutions: Recent Progress and Open Questions. *Soft Matter* **2024**, *20* (12), 2635−2687.

(12) Muthukumar, M. Anniversary Perspective: A Perspective on Polyelectrolyte Solutions. *Macromolecules* **2017**, *50* (24), 9528−9560.

(13) Dobrynin, A. V.; Rubinstein, M. Theory of Polyelectrolytes in Solutions and at Surfaces. *Prog. Polym. Sci.* **2005**, *30* (11), 1049−1118.
(14) Kharlampieva, E.; Sukhishvili, S. A. Polyelectrolyte Multilayers of Weak Polyacid and Cationic Copolymer: Competition of Hydrogen-Bonding and Electrostatic Interactions. *Macromolecules* **2003**, *36* (26), 9950−9956.
(15) Li, L.; Rumyantsev, A. M.; Srivastava, S.; Meng, S.; de Pablo, J. J.; Tirrell, M. V. Effect of Solvent Quality on the Phase Behavior of Polyelectrolyte Complexes. *Macromolecules* **2021**, *54* (1), 105−114.
(16) Takahashi, A.; Nagasawa, M. Excluded Volume of Polyelectrolyte in Salt Solutions. *J. Am. Chem. Soc.* **1964**, *86* (4), 543−548.
(17) Cannavacciuolo, L.; Sommer, C.; Pedersen, J. S.; Schurtenberger, P. S. Flexibility, and Scattering Functions of Semiflexible Polyelectrolytes with Excluded Volume Effects: Monte Carlo Simulations and Neutron Scattering Experiments. *Phys. Rev. E* **2000**, *62* (4), 5409−5419.
(18) Fixman, M.; Skolnick, J. Polyelectrolyte Excluded Volume Paradox. *Macromolecules* **1978**, *11* (5), 863−867.
(19) Wang, Z.-G. 50th Anniversary Perspective: Polymer Conformation—A Pedagogical Review. *Macromolecules* **2017**, *50* (23), 9073−9114.
(20) De Gennes, P. G.; Pincus, P.; Velasco, R. M.; Brochard, F. Remarks on Polyelectrolyte Conformation. *J. Phys.* **1976**, *37* (12), 1461−1473.
(21) Volk, N.; Vollmer, D.; Schmidt, M.; Oppermann, W.; Huber, K. Conformation and Phase Diagrams of Flexible Polyelectrolytes. In *Polyelectrolytes with Defined Molecular Architecture II*, Schmidt, M.; Springer: Berlin Heidelberg: Berlin, Heidelberg, 2004; pp. 29−65. .
(22) Borkovec, M.; Koper, G. J. M.; Piguet, C. Ion Binding to Polyelectrolytes. *Curr. Opin. Colloid Interface Sci.* **2006**, *11* (5), 280−289.
(23) Blanco, P. M.; Madurga, S.; Mas, F.; Garcés, J. L. Effect of Charge Regulation and Conformational Equilibria in the Stretching Properties of Weak Polyelectrolytes. *Macromolecules* **2019**, *52* (21), 8017−8031.
(24) Flory, P. J. *Principles of Polymer Chemistry*; Cornell university press, 1953.
(25) Nordmeier, E.; Dauwe, W. Studies of Polyelectrolyte Solutions II. The Second Virial Coefficient and the Persistence Length. *Polym. J.* **1992**, *24* (3), 229−238.
(26) Dobrynin, A. V.; Colby, R. H.; Rubinstein, M. Scaling Theory of Polyelectrolyte Solutions. *Macromolecules* **1995**, *28* (6), 1859−1871.
(27) Nordmeier, E. Studies of Polyelectrolyte Solutions IV. Effects of Ionic Strength on the Effective Polyion Charge. *Polym. J.* **1993**, *25* (1), 19−30.
(28) Fixman, M. Electrostatic Persistence Length. *J. Phys. Chem. B* **2010**, *114* (9), 3185−3196.
(29) Kitano, T.; Taguchi, A.; Noda, I.; Nagasawa, M. Conformation of Polyelectrolyte in Aqueous Solution. *Macromolecules* **1980**, *13* (1), 57−63.
(30) Sommer, C.; Pedersen, J. S.; Egelhaaf, S. U.; Cannavacciuolo, L.; Kohlbrecher, J.; Schurtenberger, P. Wormlike Micelles as "Equilibrium Polyelectrolytes": Light and Neutron Scattering Experiments. *Langmuir* **2002**, *18* (7), 2495−2505.
(31) Borue, V. Y.; Erukhimovich, I. Y. A Statistical Theory of Weakly Charged Polyelectrolytes: Fluctuations, Equation of State and Microphase Separation. *Macromolecules* **1988**, *21* (11), 3240−3249.
(32) Moussaid, A.; Schosseler, F.; Munch, J. P.; Candau, S. J. Structure of Polyacrylic Acid and Polymethacrylic Acid Solutions: A Small Angle Neutron Scattering Study. *J. Phys. II France* **1993**, *3* (4), 573−594.
(33) Svaneborg, C.; Pedersen, J. S. Monte Carlo Simulations and Analysis of Scattering from Neutral and Polyelectrolyte Polymer and Polymer-like Systems. *Curr. Opin. Colloid Interface Sci.* **2004**, *8* (6), 507−514.
(34) Ullner, M.; Staikos, G.; Theodorou, D. N. Monte Carlo Simulations of a Single Polyelectrolyte in Solution: Activity Coefficients of the Simple Ions and Application to Viscosity Measurements. *Macromolecules* **1998**, *31* (22), 7921−7933.
(35) Chu, B.; Hsiao, B. S. Small-Angle X-Ray Scattering of Polymers. *Chem. Rev.* **2001**, *101* (6), 1727−1762.
(36) Ballauff, M. SAXS and SANS Studies of Polymer Colloids. *Curr. Opin. Colloid Interface Sci.* **2001**, *6* (2), 132−139.
(37) Russo, P. S.; Streletzky, K. A.; Huberty, W.; Zhang, X.; Edwin, N. Chapter 13 - Characterization of Polymers by Static Light Scattering. In *Molecular Characterization of Polymers*, Malik, M. I.; Mays, J.; Shah, M. R. eds., Elsevier; 2021, pp. 499−532.
(38) Schurtenberger, P.; Oberdisse, J. Contrast & Contrast Variation in Neutron, X-ray and Light Scattering. In *Neutrons, X-rays, and Light: Scattering Methods Applied to Soft Condensed Matter*; Lindner, P., Oberdisse, J., Eds.; Elsevier, 2025; pp 151−181.
(39) Kratky, O.; Porod, G. Diffuse Small-Angle Scattering of x-Rays in Colloid Systems. *J. Colloid Sci.* **1949**, *4* (1), 35−70.
(40) Pedersen, J. S.; Gerstenberg, M. C. Scattering Form Factor of Block Copolymer Micelles. *Macromolecules* **1996**, *29* (4), 1363−1365.
(41) Pedersen, J. S.; Laso, M.; Schurtenberger, P. Monte Carlo Study of Excluded Volume Effects in Wormlike Micelles and Semiflexible Polymers. *Phys. Rev. E* **1996**, *54* (6), R5917−R5920.
(42) Gupta, A. M.; Edwards, S. F. Chain Conformations of Liquid-Crystalline Polymers. *Polymer* **1993**, *34* (14), 3112−3114.
(43) Danielsen, S. P. O.; Bridges, C. R.; Segalman, R. A. Chain Stiffness of Donor−Acceptor Conjugated Polymers in Solution. *Macromolecules* **2022**, *55* (2), 437−449.
(44) Kuei, B.; Gomez, E. D. Chain Conformations and Phase Behavior of Conjugated Polymers. *Soft Matter* **2017**, *13* (1), 49−67.
(45) Murnen, H. K.; Rosales, A. M.; Dobrynin, A. V.; Zuckermann, R. N.; Segalman, R. A. Persistence Length of Polyelectrolytes with Precisely Located Charges. *Soft Matter* **2013**, *9* (1), 90−98.
(46) Mykhaylyk, O. O. General Theorems, Differential Scattering Cross-Section, and Initial Data Treatment. In *Neutrons, X-rays, and Light: Scattering Methods Applied to Soft Condensed Matter*; Lindner, P., Oberdisse, J., Eds.; Elsevier, 2025; pp 19−59.
(47) Kuhn, W. B. Z. M. Statistischer Molekülgestalt Und Elastischen Eigenschaften Hochpolymerer Stoffe. *Kolloid-Z.* **1936**, *76* (3), 258−271.
(48) De Stefano, A. J.; Mengel, S. D.; Bates, M. W.; Jiao, S.; Shell, M. S.; Han, S.; Segalman, R. A. Control over Conformational Landscapes of Polypeptoids by Monomer Sequence Patterning. *Macromolecules* **2024**, *57* (4), 1469−1477.
(49) Thompson, C. J.; Ryan, A. J. Introduction to Polymers: Static Scattering. In *Neutrons, X-rays, and Light: Scattering Methods Applied to Soft Condensed Matter*; Lindner, P., Oberdisse, J., Eds.; Elsevier, 2025; pp 285−310.
(50) Cannavacciuolo, L.; Pedersen, J. S.; Schurtenberger, P. Monte Carlo Simulation Study of Concentration Effects and Scattering Functions for Polyelectrolyte Wormlike Micelles. *Langmuir* **2002**, *18* (7), 2922−2932.
(51) Pedersen, J. S.; Schurtenberger, P. Scattering Functions of Semiflexible Polymers with and without Excluded Volume Effects. *Macromolecules* **1996**, *29* (23), 7602−7612.
(52) Sharp, P.; Bloomfield, V. A. Light Scattering from Wormlike Chains with Excluded Volume Effects. *Biopolymers* **1968**, *6* (8), 1201−1211.
(53) Schweizer, K. S.; Curro, J. G. PRISM Theory of the Structure, Thermodynamics, and Phase Transitions of Polymer Liquids and Alloys. In *Atomistic Modeling of Physical Properties*, Lucien, M.; Suter, U. W.; Springer: Berlin, Heidelberg, 1994; pp. 319−377.
(54) Hayter, J. B.; Penfold, J. An Analytic Structure Factor for Macroion Solutions. *Mol. Phys.* **1981**, *42* (1), 109−118.
(55) Pedersen, J. S.; Schurtenbercer, P. Scattering Functions of Semidilute Solutions of Polymers in a Good Solvent. *J. Polym. Sci. B Polym. Phys.* **2004**, *42* (17), 3081−3094.
(56) Nová, L.; Štěpánek, M.; Morozova, I.; Tošner, Z.; Uhlík, F. Ionization and Chain Size of Weak Polyelectrolytes in Semidilute Regime. *Macromolecules* **2025**, *58* (18), 9962−9971.

https://doi.org/10.1021/acs.macromol.6c00697
Macromolecules XXXX, XXX, XXX−XXX

(57) Chiefari, J.; Chong, Y. K.; Ercole, F.; Krstina, J.; Jeffery, J.; Le, T. P. T.; Mayadunne, R. T. A.; Meijs, G. F.; Moad, C. L.; Moad, G.; et al. Living Free-Radical Polymerization by Reversible Addition−Fragmentation Chain Transfer: The RAFT Process. *Macromolecules* **1998**, *31* (16), 5559−5562.
(58) Odian, G. *Principles of Polymerization*; Wiley, 2004.
(59) Lowe, A. B.; Billingham, N. C.; Armes, S. P. Synthesis and Characterization of Zwitterionic Block Copolymers. *Macromolecules* **1998**, *31* (18), 5991−5998.
(60) Egelhaaf, S. U.; Pusey, P. N. Dynamic Light Scattering. *Neutrons, X-rays, and Light: Scattering Methods Applied to Soft Condensed Matter*; Lindner, P., Oberdisse, J., Eds.; Elsevier, 2025; pp 211−238.
(61) Cervera Gontard, L.; Ozkaya, D.; Dunin-Borkowski, R. E. A Simple Algorithm for Measuring Particle Size Distributions on an Uneven Background from TEM Images. *Ultramicroscopy* **2011**, *111* (2), 101−106.
(62) Chen, K.; Kromin, A.; Ulmer, M. P.; Wessels, B. W.; Backman, V. Nanoparticle Sizing with a Resolution beyond the Diffraction Limit Using UV Light Scattering Spectroscopy. *Opt. Commun.* **2003**, *228* (1), 1−7.
(63) Pecora, R. Dynamic Light Scattering Measurement of Nanometer Particles in Liquids. *J. Nanopart. Res.* **2000**, *2* (2), 123−131.
(64) Förster, S.; Schmidt, M.; Antonietti, M. Static and Dynamic Light Scattering by Aqueous Polyelectrolyte Solutions: Effect of Molecular Weight, Charge Density and Added Salt. *Polymer* **1990**, *31* (5), 781−792.
(65) Förster, S.; Hermsdorf, N.; Böttcher, C.; Lindner, P. Structure of Polyelectrolyte Block Copolymer Micelles. *Macromolecules* **2002**, *35* (10), 4096−4105.
(66) Guinier, A.; Fournet, G. *Small Angle Scattering of X-Rays*; Wiley: Hoboken, NJ, USA, 1955.
(67) Everaers, R.; Grosberg, A. Y.; Rubinstein, M.; Rosa, A. Flory Theory of Randomly Branched Polymers. *Soft Matter* **2017**, *13* (6), 1223−1234.
(68) De Gennes, P. G. Collapse of a Polymer Chain in Poor Solvents. *J. Phys., Lett.* **1975**, *36* (3), 55−57.
(69) Li, B.; Madras, N.; Sokal, A. D. Critical Exponents, Hyperscaling, and Universal Amplitude Ratios for Two- and Three-Dimensional Self-Avoiding Walks. *J. Stat. Phys.* **1995**, *80* (3), 661−754.
(70) Pedersen, J. S.; Schurtenberger, P. Static Properties of Polystyrene in Semidilute Solutions: A Comparison of Monte Carlo Simulation and Small-Angle Neutron Scattering Results. *Europhys. Lett.* **1999**, *45* (6), 666.
(71) Debye, P. Molecular-Weight Determination by Light Scattering. *J. Phys. Colloid Chem.* **1947**, *51* (1), 18−32.
(72) Schulz, G. V. Über die beziehung zwischen reaktionsgeschwindigkeit und zusammensetzung des reaktionsproduktes bei makropolymerisationsvorgängen. *Z. Phys. Chem.* **1935**, *30B* (1), 379−398.
(73) Jerke, G.; Pedersen, J. S.; Egelhaaf, S. U.; Schurtenberger, P. Flexibility of Charged and Uncharged Polymer-like Micelles. *Langmuir* **1998**, *14* (21), 6013−6024.
(74) Schulz, G. V. Über die Kinetik der Kettenpolymerisationen. V. *Z. Phys. Chem.* **1939**, *43B* (1), 25−46.
(75) Zimm, B. H. The Scattering of Light and the Radial Distribution Function of High Polymer Solutions. *J. Chem. Phys.* **1948**, *16* (12), 1093−1099.
(76) Casse, O.; Shkilnyy, A.; Linders, J.; Mayer, C.; Häussinger, D.; Völkel, A.; Thünemann, A. F.; Dimova, R.; Cölfen, H.; Meier, W.; Schlaad, H.; Taubert, A. Solution Behavior of Double-Hydrophilic Block Copolymers in Dilute Aqueous Solution. *Macromolecules* **2012**, *45* (11), 4772−4777.
(77) Mendez-Alcaraz, J. M.; D'Aguanno, B.; Klein, R. Structure of Binary Colloidal Mixtures of Charged and Uncharged Spherical Particles. *Langmuir* **1992**, *8* (12), 2913−2920.
(78) Rogers, F. J.; Young, D. A. N. Thermodynamically Consistent, Integral Equation for Simple Fluids. *Phys. Rev. A* **1984**, *30* (2), 999−1007.
(79) Pedersen, J. S. Model Fitting and Simulation Techniques in Small-Angle Scattering Data Analysis. In *Neutrons, X-rays, and Light: Scattering Methods Applied to Soft Condensed Matter*; Lindner, P., Oberdisse, J., Eds.; Elsevier, 2025; pp 401−495.
(80) Manning, G. S. Limiting Laws and Counterion Condensation in Polyelectrolyte Solutions I. Colligative Properties. *J. Chem. Phys.* **1969**, *51* (3), 924−933.
(81) Netz, R. R.; Joanny, J.-F. Complexation between a Semiflexible Polyelectrolyte and an Oppositely Charged Sphere. *Macromolecules* **1999**, *32* (26), 9026−9040.
(82) Everaers, R.; Milchev, A.; Yamakov, V. The Electrostatic Persistence Length of Polymers beyond the OSF Limit. *Eur. Phys. J. E* **2002**, *8* (1), 3−14.
(83) Skolnick, J.; Fixman, M. Electrostatic Persistence Length of a Wormlike Polyelectrolyte. *Macromolecules* **1977**, *10* (5), 944−948.
(84) Odijk, T. Polyelectrolytes near the Rod Limit. *J. Polym. Sci., Polym. Phys. Ed.* **1977**, *15* (3), 477−483.
(85) Moreira, A. G.; Netz, R. R. Strong-Coupling Theory for Counter-Ion Distributions. *Europhys. Lett.* **2000**, *52* (6), 705.
(86) Naji, A.; Kanduč, M.; Forsman, J.; Podgornik, R. Perspective: Coulomb Fluids—Weak Coupling, Strong Coupling, in between and Beyond. *J. Chem. Phys.* **2013**, *139* (15), 150901.
(87) Neal, T. J.; Parnell, A. J.; King, S. M.; Beattie, D. L.; Murray, M. W.; Williams, N. S. J.; Emmett, S. N.; Armes, S. P.; Spain, S. G.; Mykhaylyk, O. O. Control of Particle Size in the Self-Assembly of Amphiphilic Statistical Copolymers. *Macromolecules* **2021**, *54* (3), 1425−1440.
(88) Dobrynin, A. V.; Rubinstein, M. Hydrophobic Polyelectrolytes. *Macromolecules* **1999**, *32* (3), 915−922.
(89) Muthukumar, M. Theory of Counter-Ion Condensation on Flexible Polyelectrolytes: Adsorption Mechanism. *J. Chem. Phys.* **2004**, *120* (19), 9343−9350.
(90) Barrat, J.-L.; Joanny, J.-F. Theory of Polyelectrolyte Solutions. *Adv. Chem. Phys.* **1996**, *94*, 1−66.
(91) Akdeniz, B.; Wood, J. A.; Lammertink, R. G. H. Diffusiophoretic Behavior of Polyelectrolyte-Coated Particles. *Langmuir* **2024**, *40* (11), 5934−5944.
(92) Yang, H.; Zheng, Q.; Cheng, R. New Insight into "Polyelectrolyte Effect. *Colloids Surf., A* **2012**, *407*, 1−8.
(93) Bollinger, J. A.; Grest, G. S.; Stevens, M. J.; Rubinstein, M. Overlap Concentration in Salt-Free Polyelectrolyte Solutions. *Macromolecules* **2021**, *54* (21), 10068−10073.
(94) Essafi, W.; Lafuma, F.; Williams, C. E. Effect of Solvent Quality on the Behaviour of Highly Charged Polyelectrolytes. *J. Phys. II France* **1995**, *5* (9), 1269−1275.
(95) Plazzotta, B.; Diget, J. S.; Zhu, K.; Nyström, B.; Pedersen, J. S. Small-Angle X-Ray Scattering as a Useful Supplementary Technique to Determine Molecular Masses of Polyelectrolytes in Solution. *J. Polym. Sci. B Polym. Phys.* **2016**, *54* (19), 1913−1917.
(96) Schweins, R.; Hollmann, J.; Huber, K. Dilute Solution Behaviour of Sodium Polyacrylate Chains in Aqueous NaCl Solutions. *Polymer* **2003**, *44* (23), 7131−7141.
(97) Abou Hamad, N.; Akintola, J.; Schlenoff, J. B. Quantifying Hydrophilicity in Polyelectrolytes and Polyzwitterions. *Macromolecules* **2025**, *58* (7), 3422−3430.
(98) Sorci, G. A.; Reed, W. F. Effect of Valence and Chemical Species of Added Electrolyte on Polyelectrolyte Conformations and Interactions. *Macromolecules* **2004**, *37* (2), 554−565.
(99) Saha, S.; Fischer, K.; Muthukumar, M.; Schmidt, M. Apparent Molar Mass of a Polyelectrolyte in an Organic Solvent in the Low Ionic Strength Limit As Revealed by Light Scattering. *Macromolecules* **2013**, *46* (20), 8296−8303.
(100) Andreeva, L.N.; Bushin, S.V.; Bezrukova, M.A.; Nekrasova, T.N.; Imanbaev, R.T.; Pautov, V.D.; Nazarova, O.V.; Zolotova, Y.I.; Panarin, E.F. Conformation Properties of Poly(N,N-Dimethylami-

https://doi.org/10.1021/acs.macromol.6c00697
Macromolecules XXXX, XXX, XXX−XXX

noethyl Methacrylate) Macromolecules in Various Solvents. *Russ. J. Appl. Chem.* **2012**, *85* (3), 417−425.
(101) Flory, P. J. *Statistical Mechanics of Chain Molecules*; Interscience Publishers, 1969.
(102) Wittkop, M.; Kreitmeier, S.; Göritz, D. The Collapse Transition of a Single Polymer Chain in Two and Three Dimensions: A Monte Carlo Study. *J. Chem. Phys.* **1996**, *104* (9), 3373−3385.
(103) Le Guillou, J. C.; Zinn-Justin, J. Critical Exponents for the n-Vector Model in Three Dimensions from Field Theory. *Phys. Rev. Lett.* **1977**, *39* (2), 95−98.
(104) Jang, S. S.; Çağin, T.; Goddard, W. A., III Effect of Cyclic Chain Architecture on Properties of Dilute Solutions of Polyethylene from Molecular Dynamics Simulations. *J. Chem. Phys.* **2003**, *119* (3), 1843−1854.
(105) McBride, R. J.; Miller, J. F.; Blanazs, A.; Hähnle, H.-J.; Armes, S. P. Synthesis of High Molecular Weight Water-Soluble Polymers as Low-Viscosity Latex Particles by RAFT Aqueous Dispersion Polymerization in Highly Salty Media. *Macromolecules* **2022**, *55* (17), 7380−7391.
(106) Rogers, B. A.; Okur, H. I.; Yan, C.; Yang, T.; Heyda, J.; Cremer, P. S. Weakly Hydrated Anions Bind to Polymers but Not Monomers in Aqueous Solutions. *Nat. Chem.* **2022**, *14* (1), 40−45.
(107) Cao, N.; Zhao, Y.; Chen, H.; Huang, J.; Yu, M.; Bao, Y.; Wang, D.; Cui, S. Poly(Ethylene Glycol) Becomes a Supra-Polyelectrolyte by Capturing Hydronium Ions in Water. *Macromolecules* **2022**, *55* (11), 4656−4664.
(108) Maltesh, C.; Somasundaran, P. Effect of Binding of Cations to Polyethylene Glycol on Its Interactions with Sodium Dodecyl Sulfate. *Langmuir* **1992**, *8* (8), 1926−1930.

https://doi.org/10.1021/acs.macromol.6c00697
Macromolecules XXXX, XXX, XXX−XXX